Performance evaluation of industrial waste heat driven power cycles utilizing low global warming potential working fluids

by

Zach Marshall

A thesis submitted to the Faculty of Graduate and Postdoctoral Affairs in partial fulfillment of the requirements for the degree of

Master of Applied Science

in

Sustainable Energy

Department of Mechanical and Aerospace Engineering
Carleton University
Ottawa, Ontario
January 2021

Abstract

The industrial sector is a major emitter of waste heat, and as such many opportunities exist for the implementation of waste heat recovery systems. Selecting the correct waste heat recovery system for any given application highly depends on the temperature at which waste heat is emitted. For example, although data centers are an abundant source of waste heat, emission temperatures from this industry rarely exceed 80˚C. Due to this low temperature limitation, few power cycle options are available for heat recovery. One of the most common in this regard is the heat pump assisted organic Rankine cycle. On the other end of the spectrum are cement plants which commonly emit waste heat at temperatures above 350ºC. Contrary to the case for data centers, high temperature waste heat availability at cement plants allows for multiple power cycle options to be utilized for heat recovery, the most common being the steam Rankine, organic Rankine and Kalina cycles. Although the cycles mentioned above are advantageous in many regards, most utilize high global warming potential working fluids, which are considered to be hazardous to the environment if released into the atmosphere. The main objective of this research is to evaluate the thermodynamic and economic performance of various power cycle configurations utilizing low global warming potential working fluids for waste heat recovery in both data centers and cement plants. For data center waste heat recovery, a numerical model is developed of a heat pump assisted organic Rankine cycle and scenarios are created in which the working fluids R1234yf, R1234ze, R161, and pentane are utilized assuming the system is implemented in a typical 1000-server data center located in Toronto, Ontario. For cement plant waste heat recovery, numerical models corresponding to six different transcritical carbon dioxide power cycles are developed and applied to a system that emulates the characteristics of a conventional cement plant. The Engineering Equation Solver tool is used to develop all models and conduct simulations. To determine the

economic feasibility of each power cycle configuration, a present worth analysis is conducted. For all cases, results are compared relative to those obtained using a conventional power cycle approach. In data centers, it was found that certain low global warming potential working fluids, like R161 and pentane, have similar or better thermodynamic performance than conventional working fluids when used in a heat pump assisted organic Rankine cycle system, and that these can potentially be implemented at a much lower cost than conventional data center cooling systems. In cement plants, it was determined that an inter-regenerative transcritical carbon dioxide power cycle had the highest thermodynamic and economic performance out of all configurations studied for waste heat recovery.

Preface

This integrated thesis consists of two journal articles, both of which are currently under review. Should readers wish to reference materials from this thesis, the current thesis is required to be cited. The articles in this thesis are as follows:

- **Article 1:** Z. Marshall, and J. Duquette, "A techno-economic evaluation of low global warming potential heat pump assisted organic Rankine cycle systems for data center waste heat recovery," *Energy* [Submitted]
- **Article 2:** Z. Marshall, and J. Duquette, "A performance assessment of transcritical carbon dioxide power cycles driven by waste heat from cement plants", *Applied Thermal Engineering* [Submitted]

The aforementioned articles have been adapted slightly in each corresponding chapter for ease of flow of the dissertation. The use of copyrighted material from the published articles is acknowledged as per the corresponding publisher's permissions guidelines with respect to the authors' rights.

Acknowledgements

First and foremost, I would like to thank my supervisor Prof. Jean Duquette. Your guidance, support, and especially, patience over the last three years have been instrumental in developing my skills as a researcher. I would also like to thank all my friends and family for supporting me through this whole process. I would especially like to thank my wife, Sam, for her constant support, especially during all the late nights of research and writing.

Nomenclature

Symbols

c	cost (CAD)
e	specific exergy (kJ/kg)
E	exergy (kW)
El	electricity (kW)
h	enthalpy (kJ/kg)
i	effective interest rate (%)
k	project life (years)
$\dot{m}$	mass flow rate (kg/s)
P	pressure (kPa)
Q	heat (kW)
R	revenue (CAD)
r	per unit cost of electricity (CAD/kWh)
s	entropy (kJ/kg-K)
T	temperature (K)
$\dot{W}$	work (kW)

Acronyms and abbreviations

ASHP	air-source heat pump
CAD	Canadian dollars
cl	cooling loop
CO_2	carbon dioxide
COP	coefficient of performance
EES	Engineering Equation Solver
GWP	global warming potential
hl	heating loop
HPA	heat pump assisted
HTT	high temperature turbine
IEA	International Energy Agency
IT	information technology
LTT	low temperature turbine
MTPA	metric tonnes per annum
NPC	net present cost
NPV	net present value

O&M	operation and maintenance
ORC	organic Rankine cycle
WHR	waste heat recovery

Greek letters

η	efficiency
Π	exergy destruction (kW)

Table of Contents

List of Tables

List of Figures

Chapter 1: Introduction

The global waste heat potential is currently estimated to be as high as 246 EJ on an annual basis. A large proportion of this waste heat originates from the transportation, industrial, residential, and commercial sectors [1]. The industrial sector alone accounts for approximately 32 EJ [1], with primary waste heat sources including manufacturing plants, mining operations, chemical and petrochemical plants, and large-scale telecommunication operations [2].

To minimize waste heat emissions in the industrial sector and improve overall efficiency, waste heat driven power cycles are typically integrated into existing processes. These systems provide a number of additional benefits such as reducing energy demands and minimizing environmental impacts [3, 4, 5]. However, these systems can also be costly, and require the use of refrigerants that can be harmful to the environment.

Choosing an appropriate waste heat driven power cycle for any given industrial application highly depends on the grade of the waste heat source that is technically recoverable on site. Low, medium, and high-grade waste heat sources are defined as waste heat streams that are emitted at temperatures below 100˚C, between 100-350˚C, and above 350˚C, respectively [1]. This thesis evaluates the technical, economic, and environmental performance of various power cycles comprising low global warming potential working fluids for the following industrial waste heat recovery applications that are located at opposite ends of the temperature spectrum mentioned above: low-grade waste heat recovery from data centers, and high-grade waste heat recovery from cement plants. A short description of the current status of waste heat recovery for each of these applications is provided below.

Status of waste heat recovery in data centers:

Society's growing utilization of information technology (IT) equipment and cloud-based services in recent decades has led to the widespread expansion of data processing infrastructure, commonly referred to as data centers [6]. In 2018, the International Energy Agency (IEA) estimated that data centers accounted for roughly 1% of global electricity use by end use, which equates to 713 PJ [7]. As a significant portion of this electricity is converted to heat, chiller systems are needed to ensure that data center equipment temperatures do not become so excessive as to cause system performance degradation and irreversible damage [8, 9]. The energy consumed by these chillers accounts for roughly 50% of a data center's total annual electricity requirement [10]. As a result, significantly higher quantities of energy are dissipated as waste heat to the outdoors via cooling towers [11]. Due to their high waste heat production capacity, data centers are ideally suited for coupling with energy recovery technologies like organic Rankine cycle (ORC) power plants. Heat pump assisted (HPA) ORC plants are ideal candidates for this purpose as these systems are location independent and are easily scalable in capacity [12]. HPA-ORC plants typically recover heat indirectly via a vapour compression cycle from a water loop that is connected to the data center equipment (*i.e.* water-based), or directly from the data center equipment using a refrigerant loop (*i.e*. refrigerant-based). Another simpler, although less efficient, arrangement involves recovering heat from a conventional air-source heat pump (ASHP) chiller that is integrated in the building HVAC system [13].

Status of waste heat recovery in cement plants:

Cement production plants are considered to be the largest emitters of high-grade industrial waste heat worldwide, and are estimated to produce between 96 and 155 PJ of waste heat annually [14, 15]. These plants typically include two main sources of waste heat, with temperatures ranging

from 250˚C to 400˚C, from which a portion is reused for preheating raw processed materials. The extent to which preheating occurs in these plants can have a considerable impact on the quality of the exhaust heat that may be harnessed for power generation purposes [16]. The most common cycles utilized for waste heat recovery (and power generation purposes) in cement plants are the steam Rankine cycle, the ORC, and the Kalina cycle.

1.1 Overview of waste heat recovery modelling studies

Numerical modelling studies are typically undertaken to assess the feasibility of any given power cycle. This is done so that system performance can be estimated under varying conditions without the need to build a custom system or test on an existing one, which results in more generalized conclusions. A number of modelling studies are found in the literature regarding the analysis of power cycles for waste heat recovery in both data centers and cement plants. A review of the literature surrounding each of these topics is provided in the following sections.

1.1.1 Power cycles for waste heat recovery in data centers

Very few studies have been conducted to assess the impacts of utilizing HPA-ORC plants for energy recovery in data centers. Ebrahimi et al. [17] reviewed various data center cooling technologies and waste heat recovery technologies that are most effective for low temperature applications. They found that compared to other common heat recovery technologies like district heating, power plant co-location, and biomass co-location, the ORC is the most thermodynamically and economically promising for the three main cooling technologies considered (*i.e.* air, water, and refrigerant-based). In a separate study, focused entirely on the refrigerant-based HPA-ORC for heat recovery in data centers [18], the same authors compared the 1st and 2nd law efficiencies, and coefficient of performance (COP) of the cycles using different

working fluids, and investigated the effects of temperature variations at different locations in the plant, such as the server heat exchanger, the intermediate heat exchanger, and the ORC condenser. They found that when these system parameters are optimized, and plant costs are considered, a payback period of 3 to 8 years can be expected, depending on local electricity rates in the jurisdiction of study. Feng et al. [19] assessed the impacts of using a HPA-ORC plant for recovering low-temperature waste heat in a number of applications. They found that they could improve the cycle efficiency considerably by varying the operating conditions and selecting an appropriate working fluid. They also found that, if properly designed, a HPA-ORC plant is capable of outputting more net power than an identical ORC plant where a heat pump is not used.

The studies mentioned above assess the technical performance of various data center HPA-ORC plant configurations that operate at steady state and utilize a number of different refrigerants. These studies, however, do not consider the refrigerant's global warming potential (GWP) as a key criterion for measuring the system's environmental impact. The GWP quantifies a gas' ability to trap heat in the atmosphere over a specified period of time as compared to carbon dioxide, which is assigned a GWP of 1 [20]. For example, a molecule of gas with a GWP of 800 will trap 800 times more heat in the atmosphere than a molecule of carbon dioxide. Since energy conversion systems such as heat pumps are known to leak over their lifetime [21], it is of utmost importance to keep the refrigerant GWP as low as possible to mitigate potential undesirable environmental impacts. This is especially true given that the heat pump market has grown by 10% in the last year, and this trend is expected to continue in the same vein for years to come [22, 23]. There is currently little information available regarding the techno-economic feasibility of incorporating low GWP refrigerants in data center HPA-ORC systems. Additionally, as the HPA-ORC plant configurations in the studies mentioned above are assumed to operate at steady-state, no consideration is given to

their feasibility under real-world conditions (*i.e.* as the data center server utilization changes as a function of time).

1.1.2 Power cycles for waste heat recovery in cement plants

Amiri Rad and Mohammadi [24] designed a steam Rankine cycle plant for power generation from waste heat recovery in a cement factory located in Iran, and analyzed its performance. They developed a thermodynamic model of the system and used it to optimize both the energetic and exergetic efficiencies. They found that maximum efficiencies of 39% and 16% could be obtained, respectively. Furthermore, they found that the greatest exergy losses occurred in the evaporator. In a similar study, Ahmed et al. [25] developed a design methodology for using Rankine cycles for waste heat recovery in cement plants, but used R134a as a working fluid instead of water, opting for an ORC instead of a steam cycle. Using data from a local cement factory, they designed the cycle to maximize heat exchanger effectiveness and energetic system efficiency, and obtained values of up to 93% and 20%, respectively. Unlike the previous study, they found that the turbine was the largest source of exergy loss. In addition to steam and organic Rankine cycles, Barbosa Junior et al. [26] evaluated the Kalina cycle for electricity generation from the exhaust gases of a Brazilian cement factory. The cycle was designed to maximize the net power output, thermal and exergetic efficiencies, and the electrical capacity cost. Their results showed performance values of 2430 kW, 23.3%, 47.8%, and 1267 CAD/kW, respectively. Rather than looking at various cycles in isolation, Karellas et al. [27] compared the thermodynamic performance of a steam Rankine cycle and ORC using isopentane as a working fluid for recovering waste heat from a cement plant. Using data from a Greek cement production facility, both cycles were optimized to obtain maximum energetic and exergetic efficiencies. They found that the steam Rankine cycle was more efficient when the waste heat temperature surpassed 310˚C, however the

ORC showed better performance below this temperature. Wang et al. [28] also compared various cycles and working fluids for waste heat recovery in cement plants using typical cement plant production conditions, but provided a broader analysis by comparing the steam Rankine cycle, ORC with R123 as the working fluid, and the Kalina cycle. The genetic algorithm was used to optimize each cycle based on the exergetic efficiency. The Kalina cycle was found to be superior from a performance standpoint with an efficiency of 44.9%, compared to 36.6% for the ORC, and 42.3% for the steam Rankine cycle.

The majority of the studies described above focus on either the steam Rankine cycle, the ORC, or the Kalina cycle for power generation purposes. Steam Rankine cycles are based on mature technology, and are relatively inexpensive, however the efficiency of these cycles decreases considerably when they are used in applications where lower grade waste heat streams are available such as in cement plants. ORCs and Kalina cycles, on the other hand, perform well at low temperatures and as such are well suited for the conditions present at cement plants. The downside of these systems, however, is that they require costly working fluids (*e.g.* Isopentane, R123, R134a, and R245fa), many of which have high associated GWPs, ranging from 10 to over 1300 [29, 30, 31]. Since power cycles typically leak over their lifetime [32], the GWP of the working fluids used in these cycles is of prime importance for sustainability purposes. In order to overcome these limitations, power cycles that utilize CO_2 as the working fluid have recently been proposed as a viable alternative for waste heat recovery applications. CO_2 power cycles are advantageous relative to other power cycles as they can be optimized to operate over a wider range of input temperatures [33], and they typically occupy less space. The latter advantage is mainly a result of these systems requiring smaller components due to their high-pressure operation [34]. These systems are also advantageous as the working fluid used, CO_2, is non-toxic, non-flammable,

and non-corrosive. Moreover, CO_2 is inexpensive and abundantly available [35]. Despite its many advantages, research regarding the use of CO_2 power cycles for waste heat recovery in cement plants is limited.

Olumayegun and Wang [36] assessed the dynamic performance and control of a supercritical CO_2 power cycle for waste heat recovery in a theoretical cement plant. They developed a simulation model of the plant to demonstrate the dynamic response to changes in the waste heat temperature for a single recuperator recompression cycle and evaluate its performance. Results showed that the cycle could attain energetic efficiencies of up to 33%. In a separate study, Kizilkan [37] compared the energetic and exergetic efficiencies of a supercritical CO_2 Brayton cycle and a steam Rankine cycle for waste heat recovery in cement plants. To conduct the analysis, a numerical model was developed using data from an existing steam Rankine waste heat recovery system installed at a cement plant in Turkey. They found that the energetic and exergetic efficiencies for the CO_2 Brayton cycle were 27.6% and 58.2%, respectively, whereas these same values in the given order for the steam Rankine cycle were 24.2% and 51.4%. Although the two studies described above assess the technical impacts of using CO_2 power cycles for waste heat recovery in cement plants, very few cycles are actually analyzed, and thus no details are provided regarding the potential impacts (both technical and economic) of using different CO_2 power cycles over the range of conditions present in these facilities. Moreover, only supercritical CO_2 cycles (*i.e.* cycles in which all state points are above the critical point of CO_2) have been analyzed. No studies have been conducted that focus on transcritical CO_2 cycles for waste heat recovery in cement plants, which are better suited for the waste heat temperature ranges available at these facilities [38].

1.2 Research objectives

The major research objectives addressed in this integrated thesis are broken down by chapter as follows to address the gaps in the literature outlined in Section 1.1:

- A techno-economic evaluation of low global warming potential heat pump assisted organic Rankine cycle systems for data center waste heat recovery (Chapter 2)
    - Assess the thermodynamic performance of a refrigerant-based HPA-ORC plant utilizing four different promising low GWP refrigerants.
    - Compare the economic feasibility of two distinct data center cooling systems; a refrigerant-based HPA-ORC system, and a conventional building ASHP chiller system, that are operating under different server utilization schedules.
- A performance assessment of transcritical carbon dioxide power cycles driven by waste heat from cement plants (Chapter 3)
    - Evaluate the thermodynamic performance of various transcritical CO_2 power cycle configurations for waste heat recovery in cement plants.
    - Compare the economic feasibility of these cycles.

1.3 Organization of thesis

The remainder of this integrated thesis consists of two main body chapters on (1) waste heat driven power cycles in data center, and (2) waste heat driven power cycles in cements plants, followed by a summary of research contributions, a list of recommendations and areas for future work, and a conclusion. Each chapter is outlined briefly below:

Chapter 2: This chapter analyses the use of low GWP working fluids in a HPA-ORC for waste heat recovey (WHR) in data centers. The study evaluates the first law efficiency and coefficient of

performance (COP) of various low GWP working fluids in the WHR cycles and compares the results to more commonly used working fluids, which have much greater GWPs. For each working fluid, three theoretical data center utilization scenarios are considered, ranging from low to high server utilization, to determine if the present worth of the systems are substantial enough to encourage the implementation of an HPA-ORC system instead of the traditional computer room air conditioner system.

Chapter 3: This chapter examines the thermodynamic performance of transcritical carbon dioxide power cycles for WHR in cement plants. The energetic and exergetic efficiencies of six different cycle configurations are compared to determine the most appropriate cycle for this application and to underline which components are most and least favourable in this context. An economic analysis is also completed to determine if the present worth of the system justifies the additional costs of purchasing, installing, and operating a WHR system.

Chapter 4-6: These chapters summarize and outline key research contributions, future research work and recommendations, and conclusions, respectively.

Chapter 2

This chapter has been submitted for publication as:

Z. Marshall, and J. Duquette, "A techno-economic evaluation of low global warming potential heat pump assisted organic Rankine cycle systems for data center waste heat recovery," *Energy* [Submitted]

Chapter 2: A techno-economic evaluation of low global warming potential heat pump assisted organic Rankine cycle systems for data center waste heat recovery

2.1 Introduction

In order to address the objectives outlined in Chapter 1, a thermodynamic analysis is conducted to measure and compare power cycle performance using the refrigerants R1234yf, R1234ze, R161, and pentane with common working fluids like R134a and R245fa with respect to the system 1st law efficiency and COP. Moreover, an economic analysis is conducted to compare the feasibility of two distinct data center cooling systems; a refrigerant-based HPA-ORC system, and a conventional building ASHP chiller system, with respect to the net system electricity consumption and net present cost (NPC). Three server utilization scenarios are considered representing low, average, and high mean server power consumption. The economic analysis is conducted for a typical 1000-server data center located in Toronto, Ontario.

2.2 Methodology

2.2.1 Analysis tool

The Engineering Equation Solver (EES) tool [39] is used to construct the thermodynamic models in the current study. EES can be used to solve non-linear algebraic, differential, and integral equations. It contains a thermodynamic property database which allows for accurate thermodynamic modelling of ORC and heat pump cycles using various working fluids. The tool also tracks various values, such as temperature, enthalpy, entropy, and pressure, and plots property

curves that can be overlaid with cycle states to indicate how values vary throughout any given cycle [39]. EES has been used in numerous studies to model a variety of technologies such as a molten carbonate fuel cell [40], a bio-fueled compression ignition engine [41], an industrial steam cycle [42], a cascaded absorption-compression heat pump [43], and a solar driven trigeneration system using heat pump and ORC cycles [44] .

2.2.2 Refrigerant-based HPA-ORC system

A schematic of the refrigerant-based HPA-ORC system analyzed in this study is shown in Figure 2.1. The system functions as follows: waste heat, $Q_{evaporator}$, is recovered from a number of data center server racks (*i.e.* the evaporator) using a refrigerant as the working fluid, which delivers this heat to the intermediate heat exchanger. As this cycle additionally contains a compressor and an expansion valve, it operates as a vapour compression heat pump cycle. The intermediate heat exchanger provides heat, $Q_{intermediate}$, to the refrigerant in the ORC cycle, which is expanded in a turbine to provide useful work output, $\dot{W}_{turbine}$, in the form of electricity. This combined cycle requires electrical work input in the compressor, $\dot{W}_{compressor}$, and the pump, $\dot{W}_{pump}$, and rejects heat, $Q_{condenser}$, to the environment via a cooling tower.

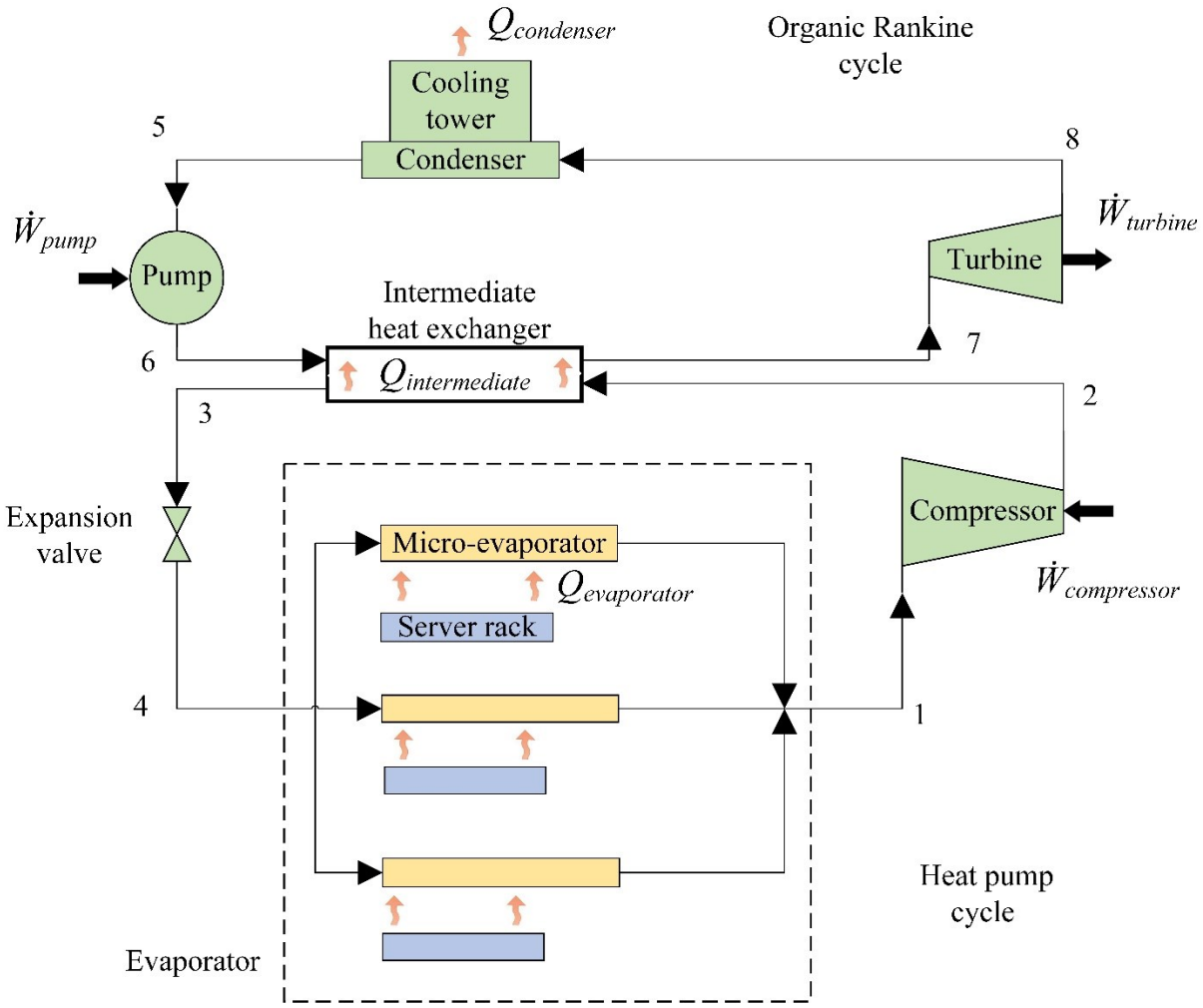

Figure 2.1: Simplified schematic of refrigerant-based HPA-ORC system for data center comprising three server racks.

The terms $Q_{evaporator}$, $Q_{intermediate}$, $Q_{condenser}$, $\dot{W}_{compressor}$, $\dot{W}_{pump}$, and $\dot{W}_{turbine}$ represent the heat recovered from individual data center server racks, the total heat sent to the ORC cycle, the heat sent to the cooling tower, the compressor electrical work input, the pump electrical work input, and the turbine electrical work output, respectively. All terms shown in Figure 2.1 are represented in units of Watts (W).

2.2.3 Thermodynamic models

Six thermodynamic models of the refrigerant-based HPA-ORC system are developed and analyzed in the current study. Each model configuration utilizes a different working fluid combination for the heat pump and ORC, as shown in Table 2.1. Table 2.2 summarizes several key thermodynamic properties for each of these working fluids (*i.e.* the molecular mass, GWP, critical temperature, and critical pressure). The first two working fluids shown in Table 2.2 are commonly used "high-GWP" refrigerants and are representative of model configuration 1. The next four working fluids are the "low-GWP" refrigerants investigated in this study. These working fluids are chosen as they have critical temperatures and critical pressures that are comparable to the working fluids used in model configuration 1, and thus are more likely to be suitable for use in existing systems without any need for major design modifications. Additionally, all four fluids have low toxicities, which reduces the safety risk when handling and using them in these systems. R1234yf and R1234ze have the lowest flammability rating, which further reduces the level of danger associated with these alternatives [45]. Overall, these refrigerants have similar or better non-thermodynamic properties than the fluids they are meant to replace.

Table 2.1: HPA-ORC model configurations and associated working fluid combinations.

Model configuration	Heat pump/ORC working fluid combination
1	R134a/R245fa
2	R1234yf/ R1234yf
3	R1234ze/ R1234ze
4	R161/ R161
5	Pentane/ Pentane
6	R161/Pentane

Table 2.2: Thermodynamic properties of working fluids [18, 45, 46, 47, 48, 49].

Working fluid	Molecular mass (kg/kmol)	GWP	Critical temperature (˚C)	Critical pressure (MPa)
R134a	102.03	1300	101	4.06
R245fa	134.05	950	154	3.64
R1234yf	114.04	4	95	3.38
R1234ze	114.04	6	110	3.64
R161	48.06	12	102	5.09
Pentane	72.15	11	197	3.37

Many of the assumptions used in this study to identify state points in model configuration 1 are based on a study conducted by Ebrahimi et al., in which a HPA-ORC model using identical working fluids is developed [18]. These assumptions are also used to develop the other model configurations in this study; however, slight modifications are required in many cases to accommodate for the particular characteristics of the different working fluids. The main assumptions are given as follows (see Figure 2.2 for reference to the location of all state points in the HPA-ORC system):

- At State 1, the working fluid is a saturated vapour and is assumed to be at a temperature of 60˚C (this temperature is slightly increased in certain instances to avoid condensation during compression);
- At State 2, the temperature is assumed to be 90˚C;
- The compressor isentropic efficiency from State 1 to State 2 is fixed at 85%;
- Heat transfer across the intermediate heat exchanger from State 2 to State 3 occurs isobarically and adiabatically (*i.e.* no heat loss to the surroundings).

- State 3 is obtained by setting the mass flow rate of the working fluid to vary linearly with the server heat input, $Q_{evaporator}$;
- The working fluid undergoes an isenthalpic expansion from State 3 to State 4 in the expansion valve;
- At State 4, the pressure is equal to that of State 1, and the working fluid is assumed to be a saturated liquid;
- At State 5, the temperature is assumed to be 20˚C and the working fluid is a saturated liquid;
- Heat transfer across the intermediate heat exchanger from State 6 to State 7 occurs isobarically and adiabatically, and the pump efficiency is fixed at 85%;
- To avoid condensation in the turbine, the temperature at State 7 is fixed such that the saturation temperature of the ORC working fluid is 5 degrees lower than the saturation temperature of the heat pump working fluid in the intermediate heat exchanger;
- At State 8, the pressure is equal to that of State 5, and the turbine efficiency is fixed at 80%;
- Local outdoor variations in temperature are not considered;
- Heat losses in the distribution system from the servers to the system are not considered;
- The cooling tower is assumed to require negligible work input; and
- The pressure losses in the system are considered to be negligible.

Temperature-entropy diagrams for each model configuration developed in this study are shown in Figure 2.2. These diagrams illustrate the temperature, pressure, quality, and entropy of the working fluid at each state in any given cycle. For the sake of clarity, model configurations that utilize the same working fluid for both heat pump and ORC cycles are overlapped in a single diagram, whereas, model configurations that utilize different working fluids for these cycles are

shown on two separate diagrams. Figure 2.2a shows the working fluid properties for the heat pump cycle utilized in model configuration 1. Due to the shape of the vapour dome, there is no risk of condensation as the working fluid goes through the compressor. Similarly, there is no risk of condensation in the turbine for R245fa (Figure 2.2b), which is the refrigerant used in the ORC in model configuration 1. Figures 2.2c and 2.2d represent model configurations 2 (R1234yf) and 3 (R1234ze), respectively. For both these cases there is no risk of condensation in the compressor, however, superheating of the working fluid is required to avoid condensation in the turbine. A similar situation is shown in Figure 2.2e, which represents model configuration 4 (R161). In this case, the shape of the vapour dome is more pronounced than those of the previous two working fluids. Figure 2.2f represents model configuration 5 (pentane), and contrary to the previous working fluids, the opposite problem occurs; that is there is no risk of condensation in the turbine, but superheating is required at State 1 to avoid condensation in the compressor. Figures 2.2g and 2.2h show the working fluid properties for the heat pump cycle (R161) and ORC (pentane) in model configuration 6, respectively. Both working fluids in this configuration have similar vapour dome shapes as many commonly used working fluids and have low risk of condensation in the compressor and turbine. One main concern associated with the use of pentane, however, is that operating pressures below atmospheric pressure are required. Design modifications may therefore be needed to avoid air infiltration in the system.

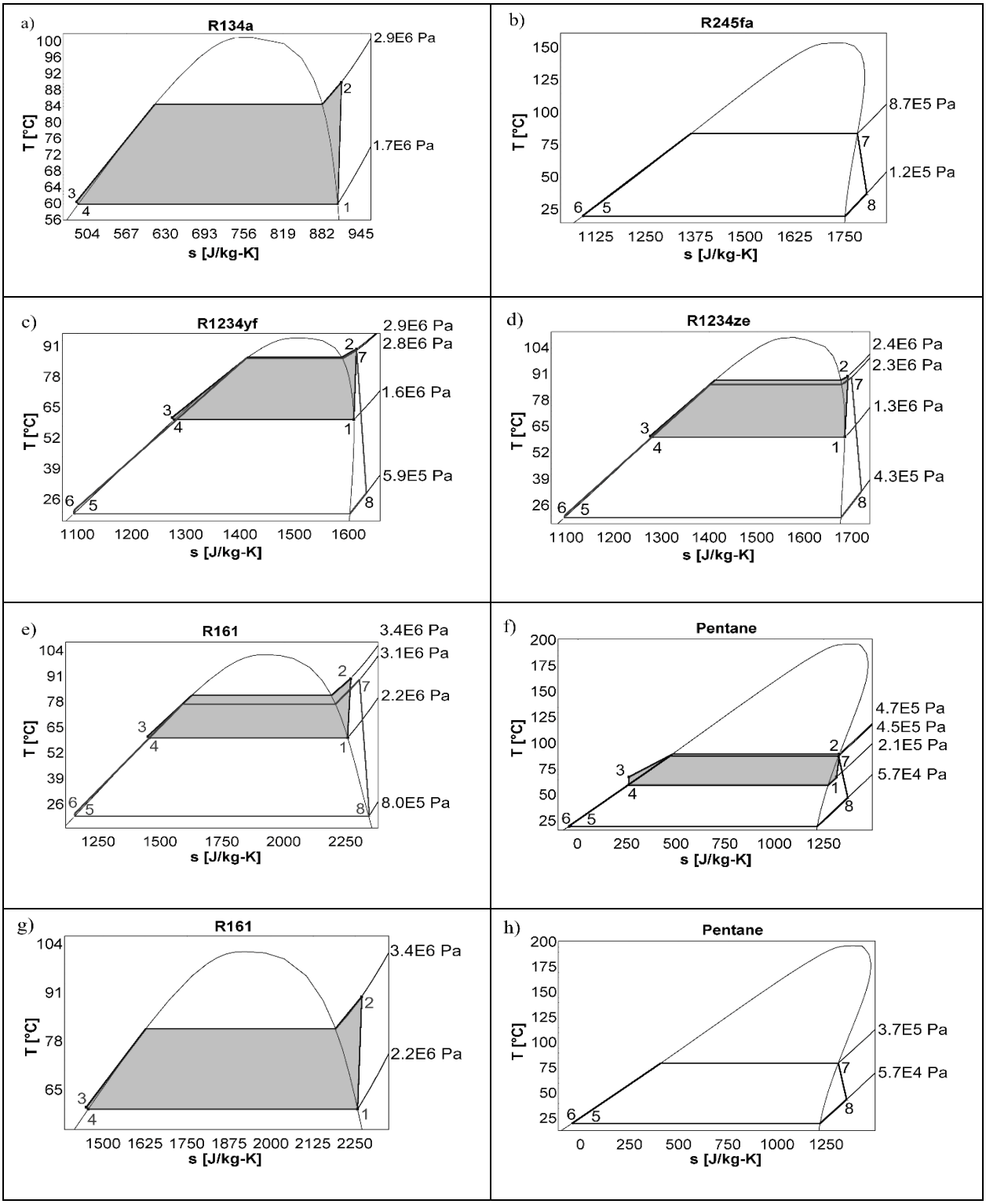

Figure 2.2 Temperature-entropy diagrams for a) Model configuration 1 - heat pump cycle (1-2-3-4) using R134a, b) Model configuration 1 – ORC (5-6-7-8) using R245fa, c) Model configuration 2 – heat pump cycle (1-2-3-4) and ORC (5-6-7-8) using R1234yf, d) Model configuration 3 - heat pump cycle (1-2-3-4) and ORC (5-6-7-8) using R1234ze, e) Model configuration 4 - heat pump cycle (1-2-3-4) and ORC (5-6-7-8) using R161, f) Model configuration 5 - heat pump cycle (1-2-3-4) and ORC (5-6-7-8) using pentane, g) Model configuration 6 – heat pump cycle (1-2-3-4) using R161, h) Model configuration 6 – ORC (5-6-7-8) using pentane.

2.2.4 Thermodynamic performance

Two metrics are used to compare the thermodynamic performance of the model configurations assessed in this study: the heat pump COP, and the system 1st law efficiency. The heat pump COP is defined as the ratio of useful heat provided by the heat pump cycle to the compressor work required to operate this cycle [50], and is expressed as

$$COP = \frac{Q_{intermediate}}{\dot{W}_{compressor}} \tag{2.1}$$

The 1st law efficiency, η, is defined as the ratio of the useful work provided by the HPA-ORC system to the heat supplied to the system, and is denoted by

$$\eta = \frac{\dot{W}_{turbine} - \left(\dot{W}_{compressor} + \dot{W}_{pump}\right)}{Q_{evaporator}} \tag{2.2}$$

2.2.5 Model verification

In order to verify the HPA-ORC numerical model, a comparison is made between the thermodynamic performance metrics obtained in the current study for model configuration 1 (*i.e.* using refrigerants R134a and R245fa for the heat pump cycle and ORC, respectively), and those obtained in a similar study conducted by Ebrahimi et al. [18]. The verification follows the assumptions listed in Section 2.2.3. The heat pump COP and system 1st law efficiency from both studies is shown in Table 2.3. This table demonstrates the thermodynamic performance metrics for both studies, with a 0.3% difference between COP values and a 0.8% difference between 1st law efficiency values.

Table 2.3: Comparison of heat pump COP and System 1st law efficiency obtained in current study and study conducted by Ebrahimi et al. (refrigerants R134a and R245fa are used for the heat pump cycle and ORC, respectively).

	Ebrahimi et al.	**Current study**
Heat pump COP	12.28	12.32
System 1st law efficiency (%)	4.70	4.74

Further verification of the numerical model (*i.e.* model configuration 1) is conducted by evaluating the impact of 1) varying the evaporator temperature on the system 1st law efficiency (Figure 2.3), and 2) varying the intermediate heat exchanger temperature on the system 1st law efficiency (Figure 2.4). In the former, a constant intermediate heat exchanger temperature of 90˚C is assumed, and in the latter a constant evaporator temperature of 60˚C is assumed. Both figures show close agreement between the current study and the Ebrahimi et al. study. The error bars represent the potential error associated with manually inputting results obtained from figures in the Ebrahimi et al. study. As the values obtained in the current study closely match those obtained by Ebrahimi et al., it can be concluded that the HPA-ORC numerical model is behaving as expected with low error. The current methodology is therefore assumed to be verified for use with model configurations 2-6.

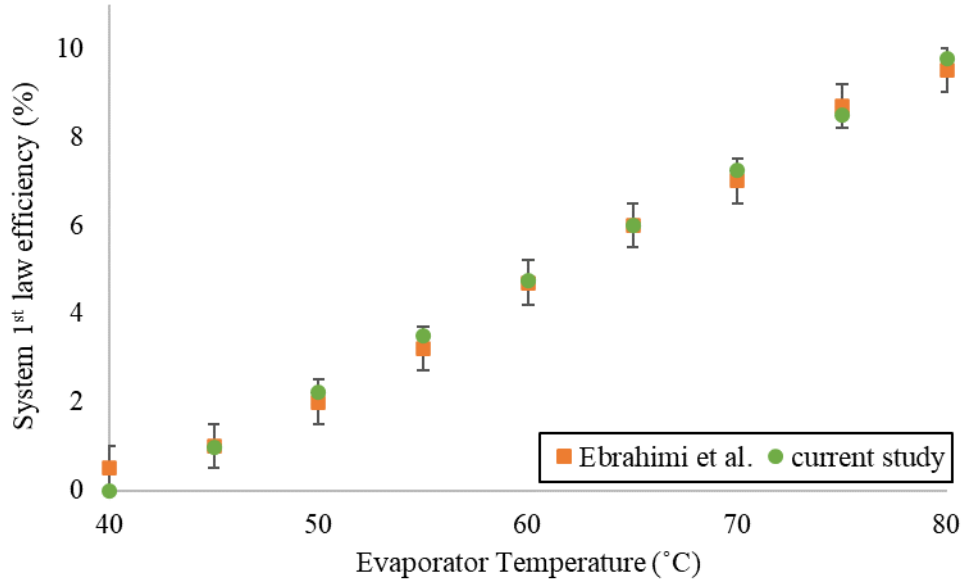

Figure 2.3: System 1st law efficiency as a function of evaporator temperature (assuming a constant intermediate heat exchanger temperature of 90˚C) for model configuration 1. Comparison between current study and Ebrahimi et al. study.

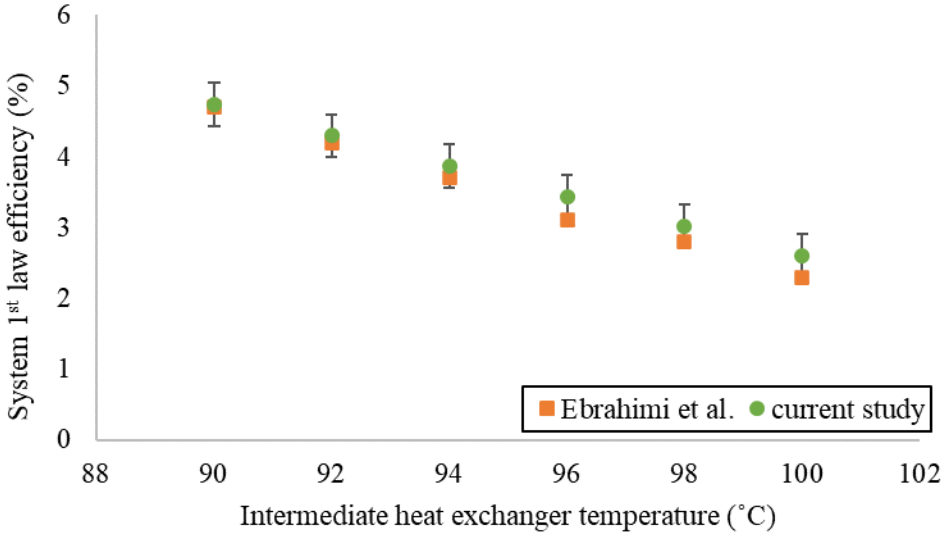

Figure 2.4: System 1st law efficiency as a function of intermediate heat exchanger temperature (assuming a constant evaporator temperature of 60˚C) for model configuration 1. Comparison between current study and Ebrahimi et al. study.

2.2.6 Data center server utilization scenarios

Three scenarios are developed to model the impact of data centers that are operating under different server utilization schedules. A data center comprising 1000 servers is assumed in the current study [51]. A typical medium-sized data center comprises approximately 1200 servers [52]. The scenarios, shown in Table 2.4, represent servers exhibiting low, average, and high mean power consumption over the course of a year. Server utilization in data centers can vary greatly, depending on the time of day, the time of year, and the purpose of the data center [53]. The mean power consumption per individual server used in this study is based on an example case from Yogendra and Pramod [51] in which they estimate a peak individual server power demand of 307 W. The low server utilization scenario shown in Table 2.4 assumes that 50% of the total data center peak power demand is consumed and represents the case where server utilization is low and/or some servers are shut down. The power consumption in this scenario is also roughly equal to the power consumed when all servers are idle [53]. The average and high server utilization scenarios assume that 65% and 80% of this peak power demand is consumed, respectively.

Table 2.4: Data center server utilization scenarios and associated mean power consumption (in W) per individual server rack.

Data center server utilization scenario	Mean power consumption per individual server (W)
Low	154
Average	200
High	246

2.2.7 Economic model

An economic analysis is conducted to compare the economic feasibility of two distinct server cooling systems in a data center located in Toronto, Ontario. These systems are a refrigerant-based HPA-ORC system (see Figure 2.1), and a conventional building air-source heat pump (ASHP) chiller system, as depicted in Figure 2.5. A comparison of these technologies is made to assess the potential economic gains from switching from a conventional ASHP chiller system to a HPA-ORC system for cooling purposes. The ASHP chiller system functions in a similar way to that of the system shown in Figure 2.1, with the following exceptions: waste heat, $Q_{evaporator_{ASHP}}$, is recovered from the air (instead of the data center server racks) via the evaporator, and no ORC cycle is utilized. Moreover, the heat supplied to the condenser, $Q_{condenser_{ASHP}}$, is rejected to the environment via a cooling tower, which requires electrical work input from the compressor, $\dot{W}_{compressor_{ASHP}}$. As in Figure 2.1, the cooling tower is assumed to require negligible work input. The terms $Q_{evaporator_{ASHP}}$, $Q_{condenser_{ASHP}}$, $\dot{W}_{compressor_{ASHP}}$, represent heat recovered from data center, heat sent to cooling tower, and compressor electrical work input, respectively. All terms shown in Figure 2.5 represent values in units of Watts (W).

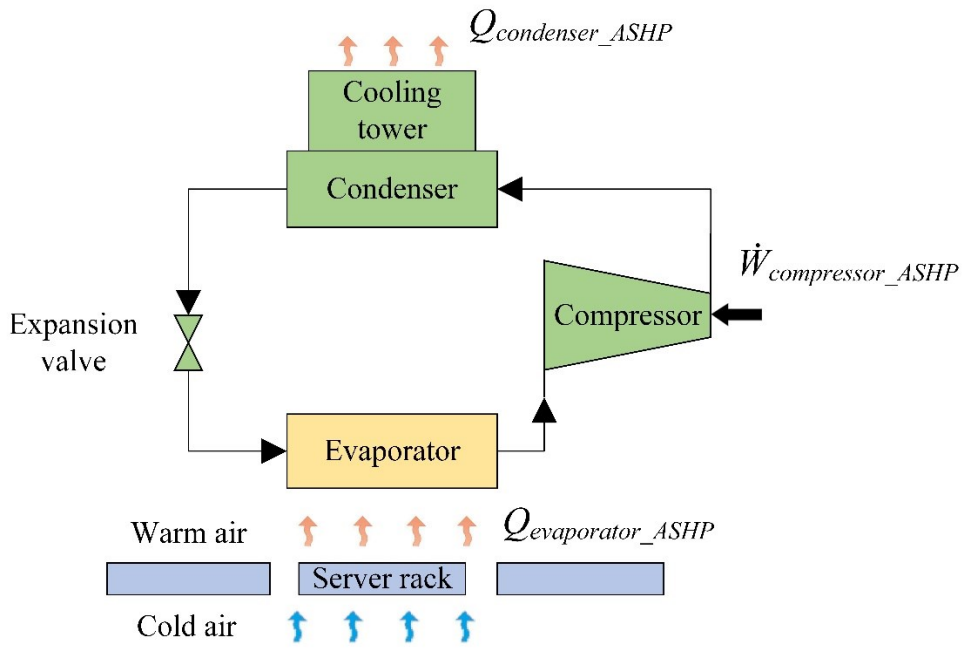

Figure 2.5: Simplified schematic of ASHP chiller system for data center comprising three server racks.

The data center utilization scenarios, described in Section 2.2.6, are used to investigate the economic impacts related to variations in server power consumption. In the current study, it is assumed that the data center cooling load is equivalent to the total server consumption [9]. As the server cooling load is assumed to be identical in both the HPA-ORC and ASHP chiller models, the following expression holds true:

$$Q_{evaporator} = Q_{evaporator\_ASHP} \tag{2.3}$$

It is also assumed that the ASHP chiller system operates with an average COP of 3 [54], which is a common value for ASHPs operating in the province of Ontario. Therefore, the net electricity consumption for the ASHP chiller system, $El_{elec_{ASHP}}$, is given by

$$El_{elec\_ASHP} = \dot{W}_{compressor\_ASHP} = \frac{Q_{evaporator\_ASHP}}{3} \tag{2.4}$$

The net electricity consumption for the HPA-ORC system, El_{elec}, on the other hand, is expressed as

$$El_{elec} = \dot{W}_{pump} + \dot{W}_{compressor} - \dot{W}_{turbine} \quad (2.5)$$

In instances where the electricity produced from the turbine exceeds the electricity consumed from the pump and compressor, it is assumed that this excess electricity is sold to the electrical grid at a fixed price.

Table 2.5 shows the component types, capacities, lifetimes, and costs associated with each of the cooling systems considered in this study. Component costs are classified into capital costs, and operation and maintenance (O&M) costs. All values are assumed to be valid for the cooling system types shown, regardless of the working fluids that are used. Each of the server cooling systems shown in Table 2.5 is sized based on the heat generated at peak server power demand, as described in section 2.2.6.

Table 2.5: Component types, capacities, lifetimes, and costs (both capital, and operation and maintenance (O&M) costs) associated with ASHP chiller, and HPA-ORC cooling systems [32, 33, 34, 35].

Data center server cooling system type	Component	Thermal Cooling Capacity (kW)	Lifetime (years)	Capital cost (k$)	O&M cost ($/year)
ASHP chiller	ASHP system	310	15	43	2,000
	Cooling tower	340	20	30	750
HPA-ORC system	HPA-ORC system	310	30	330	8,250
	Cooling tower	300	20	30	750

The net present cost (NPC) associated with each cooling system type is calculated using the formula:

$$NPC = c_c - \sum_j^k \frac{R_j - c_j}{(1+i)^j} \quad (2.6)$$

where c_c, R_j, c_j, i, j , k represent the total system capital cost, annual revenue from electricity sales (only applies to HPA-ORC system), annual O&M and electricity cost, effective interest rate, year, and project lifetime, respectively. All variables in Equation 2.6 are positive quantities. The following assumptions are taken with regards to the economic analysis: 1) the systems are built overnight, 2) an effective interest rate of 6% is used, 3) no debt is used to pay for the systems, 4) a project lifetime of 60 years is used, 5) components are replaced at the end of their useful life if this occurs within the project lifetime, 6) the components' salvage value is not considered, 7) the annual data center cooling load, and electricity cost is constant over the lifetime of the project, and 8) an average Ontario mid-peak time-of-use electricity rate of 9.4 cents/kWh is used to value electricity purchases and sales (HPA-ORC system only) from the electrical grid.

2.3 Results and Discussion

Six HPA-ORC model configurations, each comprising a different set of working fluids, are assessed from a technical and economic standpoint in the current study. A techno-economic comparison is made between the HPA-ORC model configurations and a conventional ASHP chiller. These systems are utilized for providing cooling services to a data center that is operating under three distinct server utilization scenarios. A number of insights are drawn from this assessment, which can be used to make preliminary investment decisions for new and refurbished data centers, as well as direct future research in low GWP working fluids for data center cooling systems utilizing HPA-ORC units. These insights are described as follows:

Insight 1: Low GWP working fluids like R161 and pentane demonstrate equal or better thermodynamic performance than conventional high GWP working fluids like R134a and R245fa when used in a HPA-ORC system

The heat pump COP and system 1st law efficiency of the six HPA-ORC model configurations, described in Section 2.2.3, are shown in Figure 2.6. The left axis indicates the COP values for each configuration and is associated with the red bar. The heat pump COP value is greatest in model configurations 4 and 6, with a value of 13.2, and lowest in model configurations 3 and 5, with a value of 11.4 and 11.5, respectively. The right axis indicates the system 1st law efficiency for each configuration and is associated with the blue bar. The system 1st law efficiency is greatest for model configurations 1, 5, and 6, with values of 4%, 4.1%, and 4.1%, respectively, and lowest for model configurations 2 and 3, with values of 2.4% and 2.7%, respectively. As thermodynamic performance is a factor of both heat pump COP and system 1st law efficiency, it is preferable to use a working fluid combination that maximizes these parameters. Although model configuration 6 (R161/pentane) has roughly the same system 1st law efficiency as model configuration 1 (R134a/R245fa), its heat pump COP is approximately 7% greater, making it an excellent low GWP alternative. Moreover, even though configuration 5 (pentane) has a similar system 1st law efficiency and a lower COP than configuration 1 (R134a/R245fa), pentane has a GWP of 11 while R134a and R245fa have GWPs on 1300 and 950, respectively. This reduction in GWP may potentially compensate for the slightly lower thermodynamic performance and makes pentane a comparable alternative working fluid to common fluids such as R134a and R245fa.

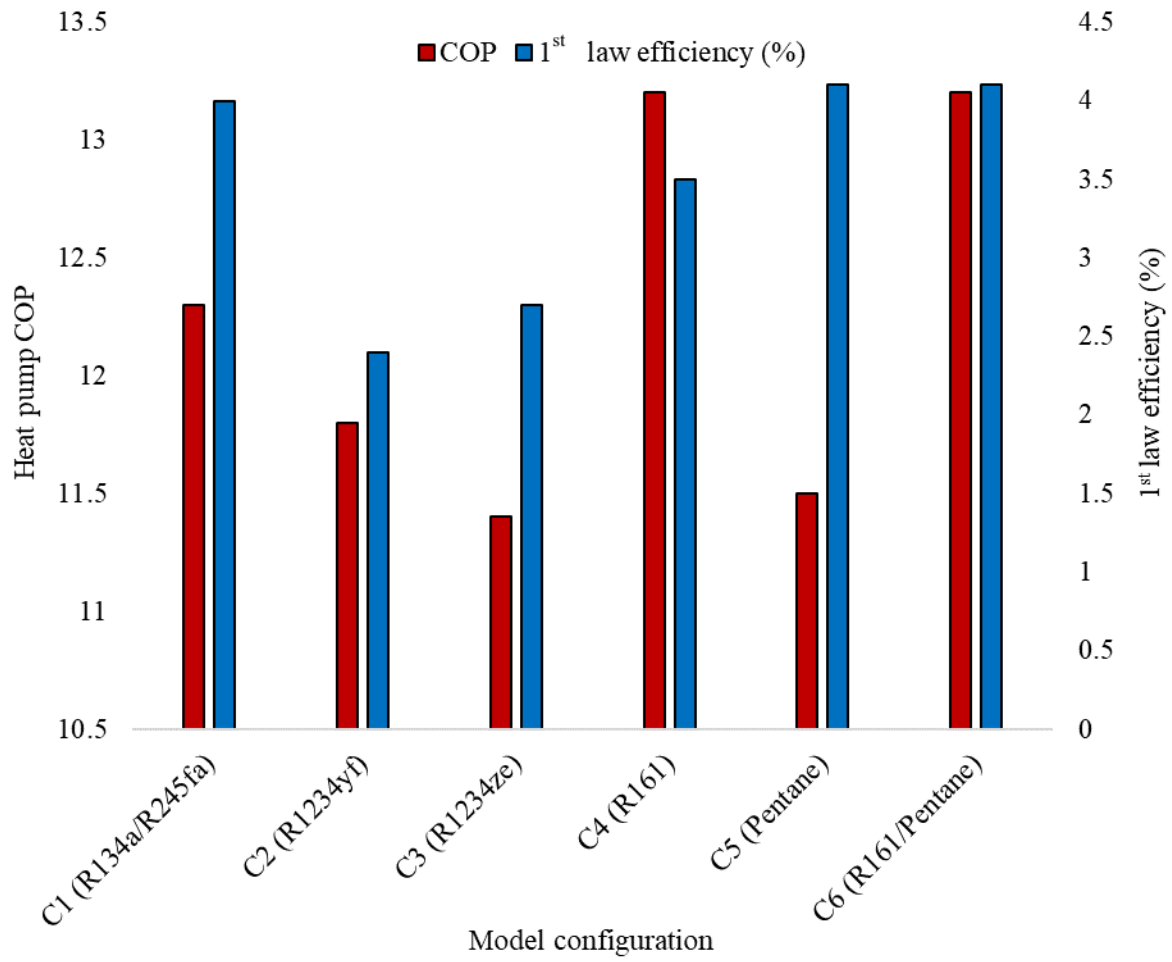

Figure 2.6: Heat pump COP and system 1st law efficiency for six HPA-ORC model configurations (C1 – C6).

Insight 2: Low GWP working fluids can potentially replace conventional (high GWP) working fluids without any need for major system modifications

The main advantage of replacing conventional working fluids like R134a and R245fa with low GWP alternatives such as R161 and pentane, respectively, aside from it being a more environmentally-friendly system, is that very few technical modifications would be required when making the switch. Figure 2.2 shows that both the conventional and low GWP working fluids considered in this study have similar state points and operating conditions. From a practical

perspective, this means that a system operator could in theory replace common working fluids like R134a and R245fa with low GWP alternatives with minimal changes to the system. The previous insight underlines that this simple replacement could result in the same or better system performance. There are however specific considerations that need to be taken into account for certain low GWP working fluids. For example, the main disadvantage of using pentane is that sub-atmospheric pressures are required in the ORC. Operating at sub-atmospheric pressures introduces a risk of air infiltration in the system, which could lead to reduced system performance or damage to system components.

Insight 3: When operating under the same conditions, all six HPA-ORC model configurations are less costly than the ASHP chiller

Figure 2.7 shows the annual net electricity consumption of each HPA-ORC configuration in comparison to the ASHP chiller. Values are provided for the three server utilization scenarios described in Section 2.2.6. The ASHP chiller consumes 455.6 MWh, 565.1 MWh, and 716.5 MWh for the low, average, and high utilization scenarios, respectively. All HPA-ORC configurations, however, produce more electricity than they consume. This electricity production varies between 32.5 MWh annually for model configuration 2 under the low server utilization scenario, and 88.9 MWh annually for model configuration 6 under the high server utilization scenario. The electricity production between the different HPA-ORC model configurations does not vary much as the system 1st law efficiency remains relatively constant in all cases, as shown in Figure 2.6.

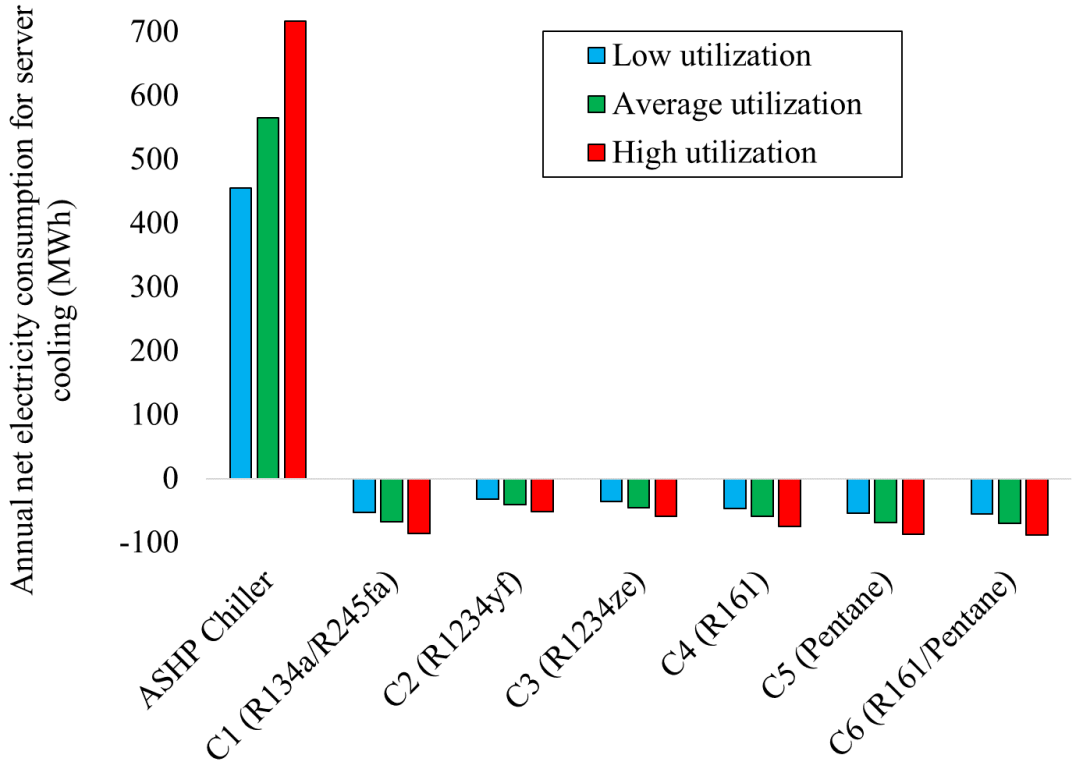

Figure 2.7: Annual net electricity consumption for server cooling for an ASHP chiller, and six HPA-ORC model configurations (C1 – C6) under three server utilization scenarios: low, average, and high.

Figure 2.8 shows the NPC of each HPA-ORC configuration in comparison to the ASHP chiller for each server utilization scenario. As electricity production exceeds electricity consumption in the HPA-ORC model configurations, and this excess electricity is sold to the grid, the NPCs of these configurations are lower than the NPC of the ASHP chiller for all server utilization scenarios. This cost reduction occurs despite the fact that the capital cost and O&M cost of the HPA-ORC system is roughly eight and four times greater than these same costs for the ASHP chiller, respectively, as shown in Table 2.5. The ASHP chiller has a NPC of $850k, $1,017k, and $1,247k for the low, average, and high utilization scenario, respectively. In comparison, the

NPCs of the HPA-ORC configurations vary from $440k for configuration 6 with a high server utilization, to $526k for configuration 2 with a low server utilization.

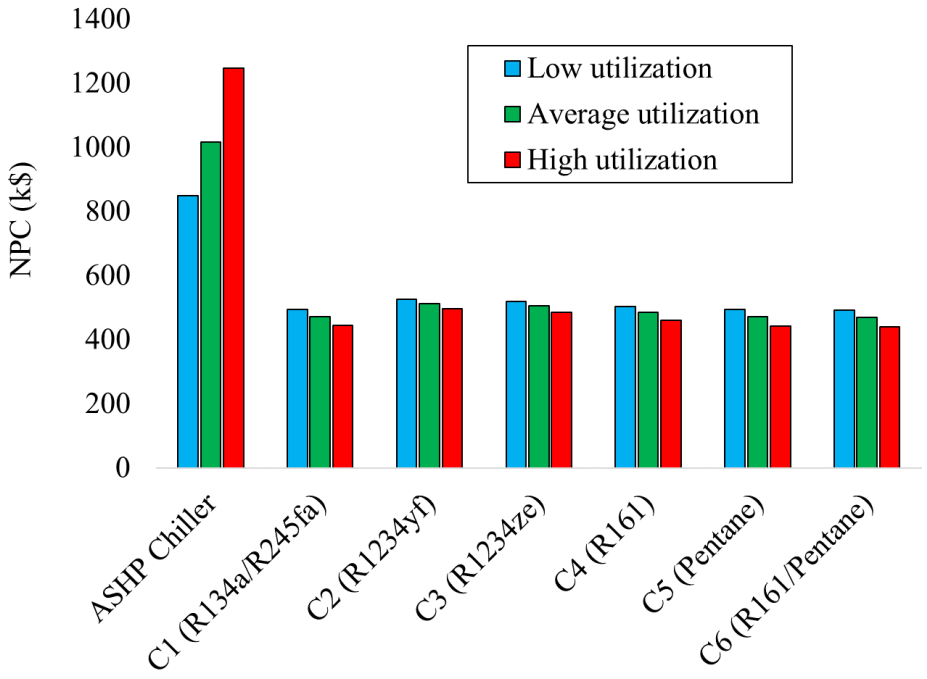

Figure 2.8: Net present cost (NPC) for an ASHP chiller, and six HPA-ORC model configurations (C1 – C6) under three server utilization scenarios: low, average, and high.

Insight 4: Relative to the ASHP chiller system, the profitability of the HPA-ORC model configurations increases as the server utilization increases

Figure 2.8 demonstrates the impact of server utilization on the NPC of both the ASHP chiller and HPA-ORC model configurations. The NPC of the ASHP chiller system increases as server utilization increases. For example, increasing utilization from low to high results in a gain in NPC of roughly $397k. This gain occurs due to an increase in electricity consumption which needs to be purchased from the electrical grid. The NPC of the HPA-ORC model configurations, on the other hand, decreases as server utilization increases. This is due to greater amounts of heat

being produced at higher utilization, which results in greater ORC electricity production, and increased power sales to the electrical grid.

Insight 5: Electricity price and discount rate have the greatest impact on the NPC of the ASHP chiller, whereas capital cost and O&M cost have the greatest impact on the NPC of the HPA-ORC model configurations

A sensitivity analysis is conducted to identify the parameters used in the study that have the greatest impact on system net present cost. The analysis is conducted on both the ASHP chiller system (Figure 2.9a), and HPA-ORC model configuration 6 (Figure 2.9b). Only one HPA-ORC model configuration is assessed as the sensitivity of the various parameters considered on the NPC is relatively uniform across all configurations. Model configuration 6 is chosen as it has the highest 1st law efficiency of the six HPA-ORC model configurations analyzed in this study. The following five technical/economic parameters are varied from a low to a high value in the analysis: server utilization, discount rate, electricity price, capital cost, and O&M cost. Additionally, a "most extreme case" parameter is varied in the analysis. The "most extreme case" parameter shows the impact on net present cost when all five parameters in Figure 2.9 are varied simultaneously in order to achieve the greatest increase and decrease. The low and high values of electricity price are taken as half (4.7 cents/kWh), and double (18.8 cents/kWh) the value used in the economic analysis, respectively. Similarly, low and high values of the discount rate are taken as 4% and 12%, based on guidelines from the Government of Canada [55]. For capital and O&M costs, values equivalent to half and double of those shown in Table 2.5 are taken as the low and high values, respectively. For server utilization, values corresponding to the low and high utilization scenarios

described in section 2.2.6 are taken as the low and high values in Figure 2.9. As these parameters are varied, the corresponding percentage increase/decrease of the net present cost is shown on the horizontal axis. For example, the low value for the discount rate results in a 38% increase in the NPC of the ASHP chiller.

Figure 2.9a shows that the ASHP chiller is highly sensitive to both the electricity price and the discount rate. The associated NPC variations of these parameters from a low to high value are equivalent to 126% and 84%, respectively. However, the system shows little sensitivity to both capital and O&M cost, as NPC variations of these parameters are roughly equivalent to 6%. Variations in capital and O&M costs do not greatly impact the ASHP chiller NPC because these costs are relatively small when compared to the annual amount spent on electricity. The opposite holds true for the HPA-ORC system. Figure 2.9b shows that the HPA-ORC system is highly sensitive to both capital and O&M cost. The associated NPC variations of these parameters from a low to high value are equivalent to 105% and 47%, respectively. Server utilization, on the other hand, has little impact on the system NPC, as demonstrated by an NPC variation from a low to high value of 41%. Varying both server utilization and electricity price have opposite effects on the system NPC when comparing the ASHP chiller to the HPA-ORC system. For example, an increase in server utilization causes an increase in the ASHP chiller NPC, whereas it causes a decrease in the HPA-ORC system NPC. Similarly, an increase in electricity price causes an increase in the ASHP chiller NPC, whereas it causes a decrease in the HPA-ORC system NPC.

The sensitivity results shown in Figure 2.9 bring to light the economic trade-offs between the ASHP chiller and HPA-ORC systems when subject to varying project environments. The jurisdiction in which such a system operates therefore has a significant impact on the type of

system that is selected, as many of the parameters considered (*i.e.* server utilization, discount rate, and electricity) are highly location dependent.

a)

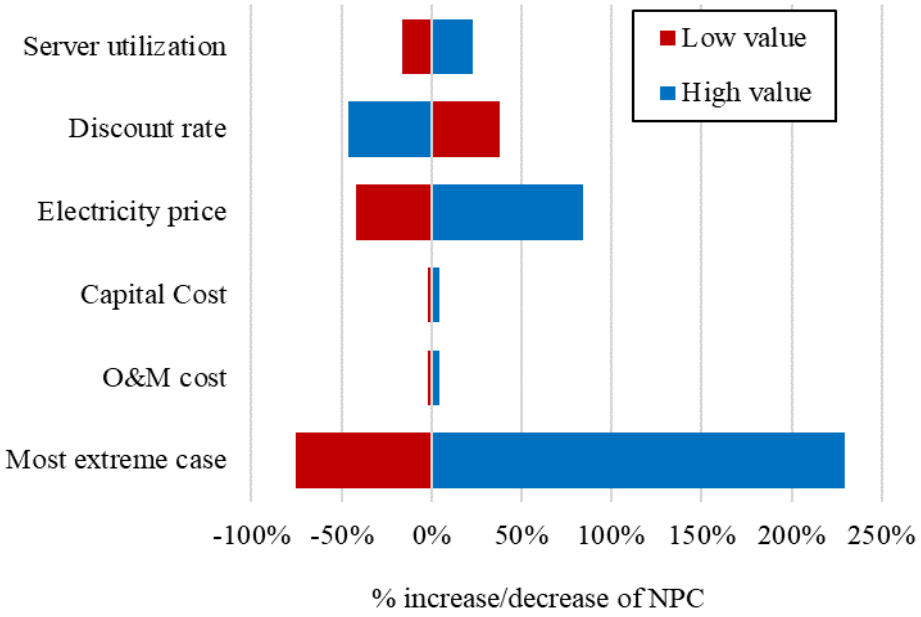

b)

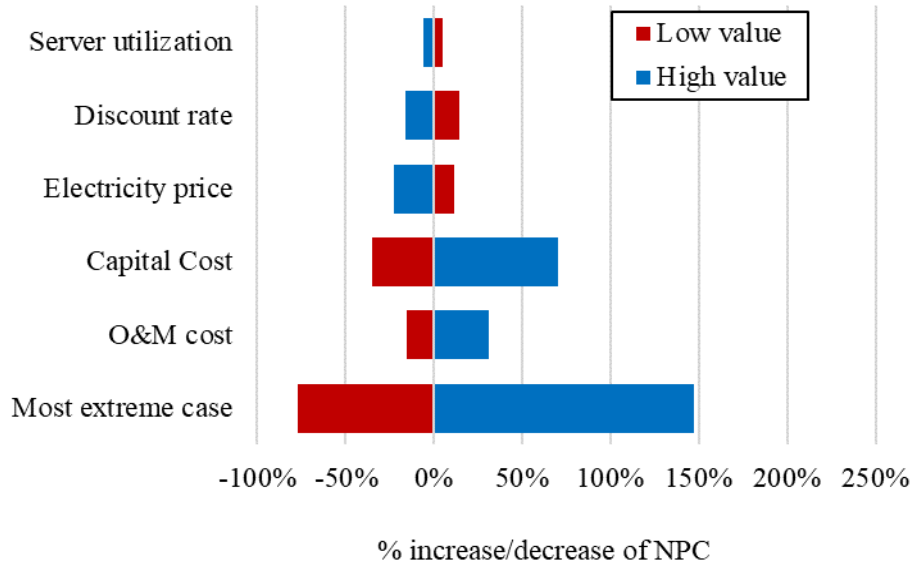

Figure 2.9: Impact of varying a number of technical and economic parameters (from a low value to a high value) on the net present cost of a) the ASHP chiller and b) HPA-ORC model configuration 6.

Insight 6: HPA-ORC systems are a lower risk investment than ASHP chillers for providing server cooling

Information regarding the stability of a particular server cooling technology investment can also be gathered from Figure 2.9. For example, the HPA-ORC system is demonstrated to be a lower risk investment than the ASHP chiller system. This is evident for the following reasons: Firstly, server utilization is more likely to increase than decrease during a project's lifetime [7], effectively decreasing the HPA-ORC system's NPC, and increasing the ASHP chiller system's NPC; Secondly, variations in discount rate and electricity price have a much lower impact on the HPA-ORC system's NPC than on the ASHP chiller system's NPC. This revelation is important as the discount rate is highly dependent on the party that is responsible for financing the server cooling project, and thus this parameter is liable to change rapidly and unpredictably at the onset of the project. Although the electricity price is considered to be an equally volatile parameter, any change in its value is likely to have a positive impact on the HPA-ORC system's NPC (*i.e.* it would result in a decrease in the NPC) as the electricity price in many jurisdictions in North America is expected to increase in the near future [56]. The opposite holds true for the ASHP chiller system; Thirdly, although the HPA-ORC system's NPC is highly sensitive to capital cost, this parameter is known at the onset of the project and as a result it cannot affect the project's economic viability once it has been initiated; Finally, the NPC variation from a low to high value for the most extreme case parameter is equivalent to 224% for the HPA-ORC system, as compared to 305% for the ASHP chiller system. The smaller sensitivity range of the HPA-ORC system demonstrates greater stability in the face of unpredictability.

2.3.1 Unresolved issues

Although the current study is useful in identifying practical insights into the server cooling technologies that have been assessed, a number of unaddressed technical issues have been identified that could serve as a starting point for future research. These issues are stated as follows:

- State points and operating conditions of the various HPA-ORC model configurations analyzed are based off of a conventional HPA-ORC chiller system comprising R134a and R245fa working fluids. Certain cycles operating with alternative working fluids such as pentane could potentially be further optimized from a performance standpoint if these assumed state points and operating conditions were varied;
- Server utilization is assumed to be constant in each server utilization scenario. A more refined approach could involve integrating historical time series usage data from an operational data center; and
- 100% effectiveness is assumed in the system heat exchangers. More realistic heat transfer conditions specific to the heat exchanger geometries and working fluids could be assessed in future work.

2.4 Conclusions

This study investigated the thermodynamic performance of refrigerant-based HPA-ORC systems utilizing various low GWP refrigerants. An economic assessment was additionally conducted to assess the feasibility of these systems when compared to a traditional ASHP chiller system. It was found that certain low GWP working fluids, like R161 and pentane, have similar or

better thermodynamic performance than conventional working fluids, like R134 and R245fa, when used in a HPA-ORC system. From an economic feasibility standpoint, it was determined that the HPA-ORC system is less costly than the ASHP chiller when operating under the same conditions for all working fluids considered. Moreover, the profitability of HPA-ORC systems increases with an increase in server utilization, while the opposite holds true for ASHP chiller systems. Both electricity price and discount rate have the greatest impact on the NPC of ASHP chiller systems, whereas capital cost and O&M costs have the greatest impact on the NPC of HPA-ORC configurations. Overall, the study showed that low GWP working fluids are a thermodynamically and economically viable alternative to conventional working fluids in data center HPA-ORC systems. Implementing these systems on a large scale has the potential to provide considerable benefits to an industry that is projected to continue growing along with our society's dependence on cloud-based IT services.

Chapter 3

This chapter has been submitted for publication as:

- Z. Marshall, and J. Duquette, "A performance assessment of transcritical carbon dioxide power cycles driven by waste heat from cement plants", *Applied Thermal Engineering* [Submitted]

Chapter 3: A performance assessment of transcritical carbon dioxide power cycles driven by waste heat from cement plants

3.1 Introduction

In order to address the objectives outlined in Chapter 1, a thermodynamic analysis is conducted to compare six transcritical CO_2 power cycle configurations with respect to the 1st and 2nd law efficiencies. Moreover, an exergy accounting framework is developed to identify primary sources of exergy destruction. Additionally, an economic analysis is conducted to determine the feasibility of each power cycle configuration with respect to the net present value. A conventional cement plant layout is used as the case study in the analysis.

3.2 Methodology

3.2.1 Case study cement plant layout

The conventional cement plant layout [24], depicted in Figure 3.1, is used as the basis from which all models are developed in the current study.

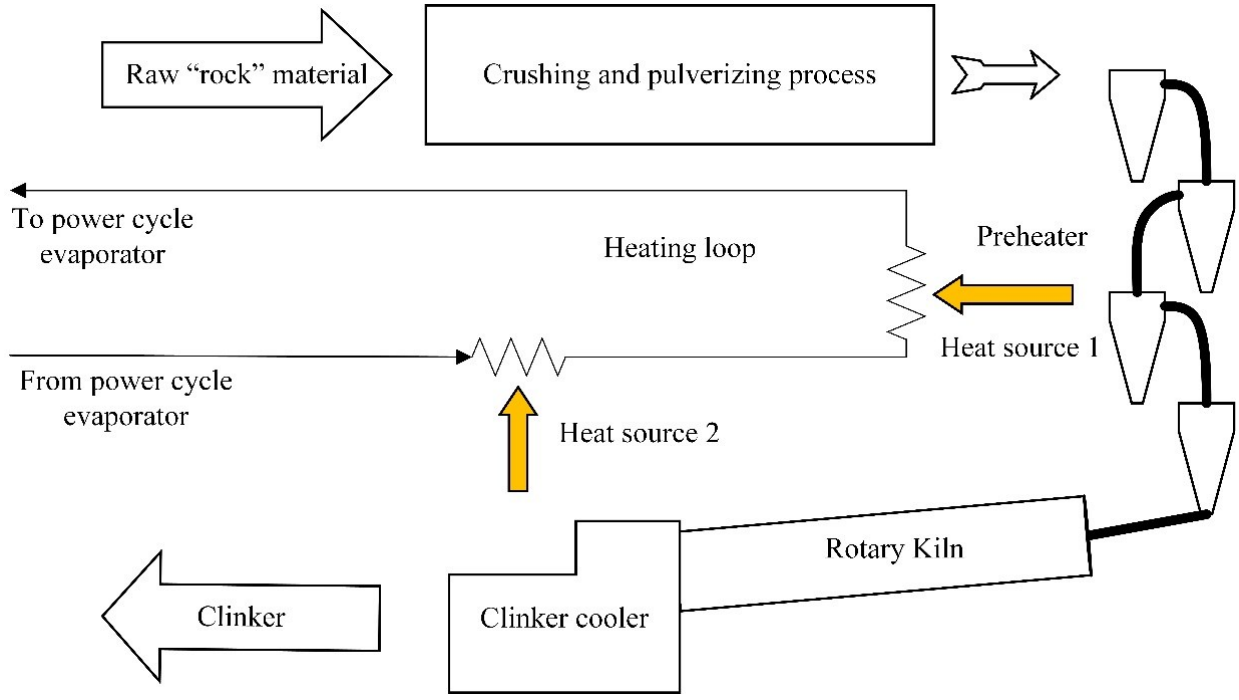

Figure 3.1: Schematic of a simplified conventional cement plant layout.

Figure 3.1 shows that the raw "rock" material starts off by entering a multi-step crushing and pulverizing process. After leaving this process, the crushed rock is heated through preheaters before entering the rotary kiln. The rotary kiln is the main heating process that transforms the crushed rock into clinker. The clinker is subsequently cooled in the "clinker cooler" and then sent out for packaging and distribution. Cement plants generally have two sources of waste heat: the preheater exhaust, and the clinker cooler exhaust, shown as "Heat source 1" and "Heat source 2", respectively, in Figure 3.1. The preheater operates at a higher temperature than the clinker cooler, therefore it is considered to be a higher-grade waste heat source. Accordingly, a cascading heating loop is considered in this study to collect the heat from these two sources (from clinker cooler to preheater) and transfer it to the evaporator of the power cycle.

3.2.2 Thermodynamic modelling framework

The following six transcritical CO_2 power cycles (see Figure 3.2) are modeled: the basic cycle, regenerative cycle, intercooling cycle, inter-regenerative cycle, split-expansion cycle, and double-stage cycle. The basic cycle comprises the four fundamental components of the power cycle: the evaporator, the turbine, the condenser, and the pump [57]. The pump increases the pressure of the working fluid prior to circulation through the evaporator, where heat is collected from the heating loop (hl) to bring the working fluid to a supercritical state. The heated supercritical CO_2 is then expanded through a turbine before being cooled in the condenser, where it returns to a subcritical state. The regenerative cycle makes use of a regenerator in addition to the components found in the basic configuration to transfer heat from the turbine output to the evaporator input [57]. The intercooling cycle is similar to the regenerative cycle, except that the cooling process occurs in two condensers and two pumps, instead of in one condenser and one pump [57]. The inter-regenerative cycle makes use of a second regenerator in addition to the components found in the regenerative cycle to maximize the heat transfer from the turbine output to the evaporator input [57]. The split-expansion cycle is similar to the regenerative cycle except it uses the transferred heat from the regenerator to operate a second turbine prior to being sent to the evaporator [57]. The double-stage cycle is the only configuration where the working fluid is separated into multiple streams [58]. A portion of the working fluid goes through a low-temperature regenerator prior to collecting heat in the evaporator and being expanded through the high-temperature turbine. The remainder of the working fluid goes through the high-temperature regenerator, collecting heat from the high-temperature turbine exhaust, which is then expanded through a low-temperature turbine. The exhaust of this turbine is used as a heat source in the low-temperature regenerator. Both flows combine again before entering the condenser.

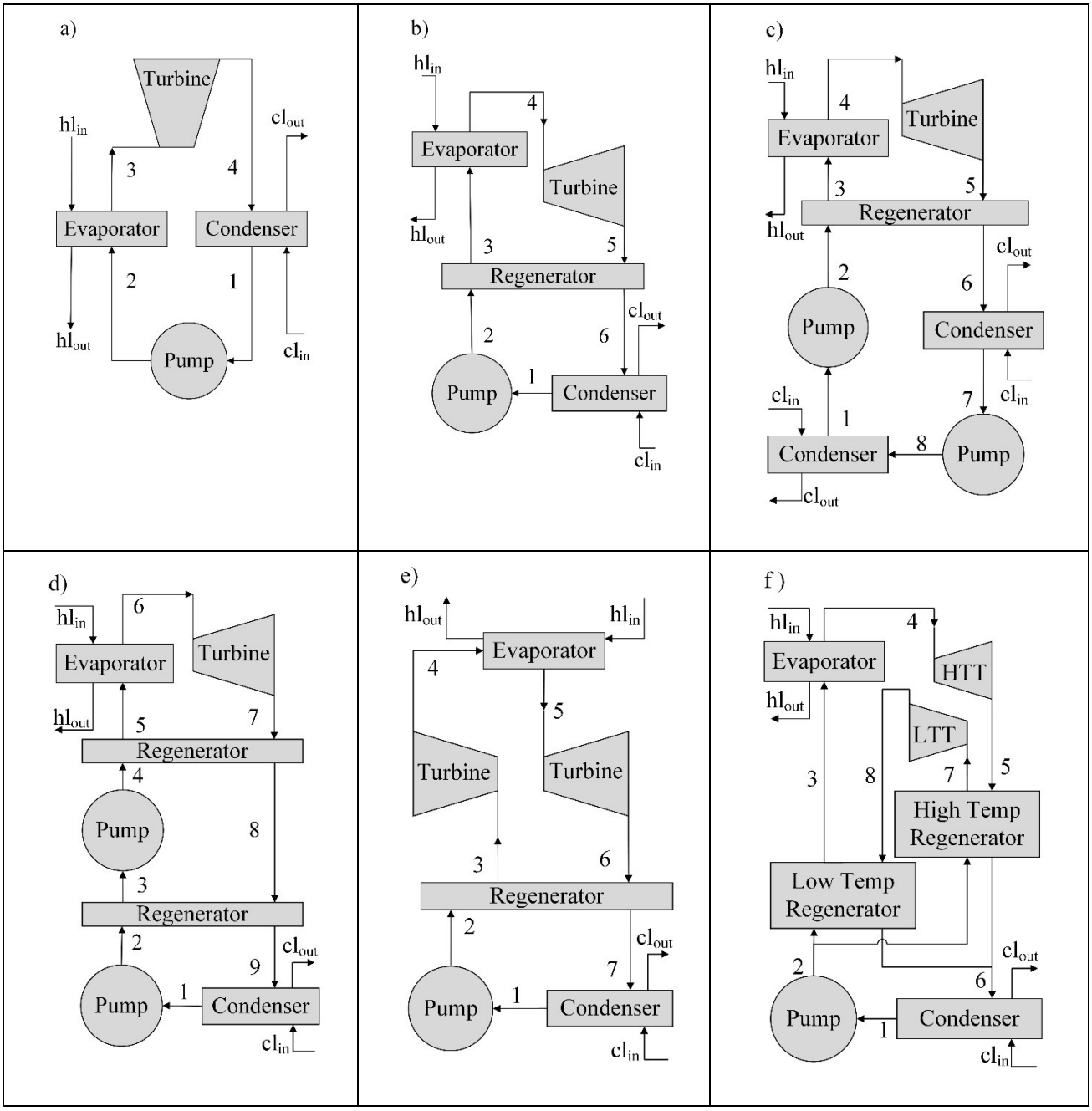

Figure 3.2: Schematic diagrams of six transcritical CO_2 power cycles driven by waste heat from a cement plant. a, b, c, d, e, and f represent the basic cycle, regenerative cycle, intercooling cycle, inter-regenerative cycle, split-expansion cycle, and double-stage cycle, respectively. hl, cl, HTT, and LTT represent heating loop, cooling loop, high temperature turbine, and low temperature turbine, respectively.

The Engineering Equation Solver (EES) tool [39] is used to model the six transcritical CO_2 power cycles considered in this study. The principal advantage of this tool is its extensive built-in database of thermodynamic properties, and responsiveness to changing operational parameters and configurations. Furthermore, it is capable of conducting parametric analyses for design optimization purposes. EES has been used in similar WHR studies related to steam Rankine [59], organic Rankine [60], and Kalina cycles [61].

A number of assumptions are taken to develop the modelling framework that is used to compare the various power cycles. For instance, although the availability and quality of waste heat are highly plant-specific in practice, the current study assumes that the plant generates one million metric tonnes of cement per annum [14], which corresponds to a waste heat potential of 94.3 GJ/hr (at a temperature of 360˚C) from the preheater, and 41.9 GJ/hr (at a temperature of 310˚C) from the clinker kiln [62]. A simplified approach is used in this study in which the temperature of the working fluid entering the evaporator from the heating loop is fixed at 355˚C for all power cycles (*i.e.* 5 degrees less than the temperature of the waste heat stream leaving the preheater). The temperature of the working fluid leaving the evaporator from the heating loop, on the other hand, is set to be 5 degrees greater than the temperature of the CO_2 entering the evaporator to avoid pinch point limitations [63]. Thus, to ensure that an equal amount of energy (*i.e.* 136.2 GJ/hr) is transferred from the heating loop to the CO_2 stream via the evaporator for all power cycles, the temperature of the heating loop working fluid leaving the evaporator, as well as its mass flow rate, is allowed to vary in each cycle. Similarly, to ensure that the required amount of heat is removed from the condenser, the temperature of the cooling loop working fluid entering the condenser is fixed at -5˚C for all cycles, and its mass flow rate is allowed to vary in each cycle. Furthermore, to avoid pinch point limitations in the condenser, the cooling loop working fluid is assumed to be

a saturated liquid as it enters the condenser and a saturated vapour as it exits the condenser. The heating loop working fluid is assume to be water pressurized at 22 MPa, whereas the cooling loop working fluid is assumed to be ammonia pressurized at 0.34 MPa. Water and ammonia are commonly used working fluids for delivering heat to and from power plant cycles [27, 64]. Pump power consumption, head losses, and heating losses/gains in both the heating and cooling loops are assumed to be negligible.

With regards to setting the state point properties of the different power cycles (see Figure 3.3 for the various configurations), the following general assumptions are taken:

- The temperature of the CO_2 leaving the evaporator is 5 degrees lower than the temperature of the working fluid entering the evaporator from the heating loop.
- The maximum allowable pressure in the system is set at 25 MPa to reduce the risk of damaging the components [65].
- Pumps have an isentropic efficiency of 85% [66].
- Turbines have an isentropic efficiency of 90% [66].
- The CO_2 leaving the condenser is assumed to be a saturated liquid to avoid condensation in the pump.
- Head losses and heat losses/gains in the piping and components are negligible.
- Specific pressure and temperature state points are selected for each cycle based on the results of a preliminary iterative analysis which consists of varying setpoints until the system's thermodynamic performance is maximized.

The work required by a pump (in kW) in any given cycle is expressed as

$$\dot{W}_p = \dot{m}(h_{out,p} - h_{in,p}) \tag{3.1}$$

where $\dot{m}$ is the mass flow rate of the working fluid (in kg/s), $h_{in,p}$ is the real enthalpy value of the working fluid entering the pump (in kJ/kg), and $h_{out,p}$ is the real enthalpy value of the working fluid exiting the pump (in kJ/kg) given by

$$h_{out,p} = h_{in,p} + \frac{h_{out,p'} - h_{in,p}}{\eta_{pump}}. \tag{3.2}$$

The variables η_{pump} and $h_{out,p'}$ in Equation 3.2 represent the pump isentropic efficiency, and the isentropic enthalpy value of the working fluid exiting the pump (in kJ/kg), respectively. Similarly, the work produced by a turbine in any given cycle is expressed as

$$\dot{W}_t = \dot{m}(h_{in,t} - h_{out,t}) \tag{3.3}$$

where $h_{in,t}$ is the real enthalpy value of the working fluid entering the turbine (in kJ/kg), and $h_{out,t}$ is the real enthalpy value of the working fluid exiting the turbine (in kJ/kg) given by

$$h_{out,t} = h_{in,t} - \eta_{turbine}(h_{in,t} - h_{out,t'}). \tag{3.4}$$

The variables $\eta_{turbine}$ and $h_{out,t'}$ in Equation 3.4 represent the turbine isentropic efficiency, and the isentropic enthalpy value of the working fluid exiting the turbine (in kJ/kg), respectively.

The net work (in kW) for any given cycle is then defined as

$$\dot{W}_{net} = \sum \dot{W}_t - \sum \dot{W}_p. \tag{3.5}$$

For all cycles, the mass flow rate of the CO_2 stream is given by

$$\dot{m} = \frac{Q_{in}}{(h_{out,e} - h_{in,e})} \tag{3.6}$$

where Q_{in}, $h_{in,e}$, and $h_{out,e}$ represent the amount of heat (in kW) transferred across the evaporator from the heating loop, the real enthalpy value (in kJ/kg) of the working fluid entering the

evaporator, and the real enthalpy value (in kJ/kg) of the working fluid exiting the evaporator, respectively.

Likewise, the heat (in kW) transferred across the condenser to the cooling loop for all cycles is expressed as

$$Q_{out} = \dot{m}(h_{in,c} - h_{out,c}) \tag{3.7}$$

where $h_{in,c}$ and $h_{out,c}$ represent the real enthalpy value (in kJ/kg) of the working fluid entering the condenser, and the real enthalpy value (in kJ/kg) of the working fluid exiting the condenser, respectively.

For cycles that include a regenerator, it is assumed that the temperature of the working fluid exiting the regenerator from the hot side is 5 degrees greater than the temperature of the working fluid entering the regenerator from the cold side to avoid pinch point limitations [67]. Based on conservation of mass, the real enthalpy value (in kJ/kg) of the working fluid exiting the regenerator on the cold side is given by

$$h_{out,cold} = h_{in,hot} - h_{out,hot} + h_{in,cold} \tag{3.8}$$

where $h_{in,cold}$ is the real enthalpy value (in kJ/kg) of the working fluid entering the regenerator from the cold stream, $h_{in,hot}$ is the real enthalpy value (in kJ/kg) of the working fluid entering the regenerator from the hot side, and $h_{out,hot}$ is the real enthalpy value (in kJ/kg) of the working fluid exiting the regenerator from the hot side, respectively. Equation 3.8 is valid for all regenerators used in single flow configurations, where the mass flow rate on both the hot and cold side is identical.

For the double-stage cycle, the flow separation ratio, x, is associated with the flow stream between the pump and the low and high temp regenerators and is expressed as

$$x = \frac{h_5 - h_6}{h_5 - h_6 + h_7 - h_2} \tag{3.9}$$

where h_2, h_5, h_6, and h_7 represent the enthalpy values (in kJ/kg) of the corresponding state points shown in Figure 3.3f. Moreover, the temperature of the working fluid at state 7 is assumed to be 10 degrees lower than the temperature at State 5 [58]. Applying the energy conservation equation to the low-temperature regenerator, the real enthalpy value (in kJ/kg) of the working fluid entering the evaporator is given by

$$h_3 = h_2 + \frac{x}{1 - x}(h_8 - h_6) \tag{3.10}$$

where h_2, and h_8 represent the enthalpy values (in kJ/kg) of the corresponding state points shown in Figure 3.3f.

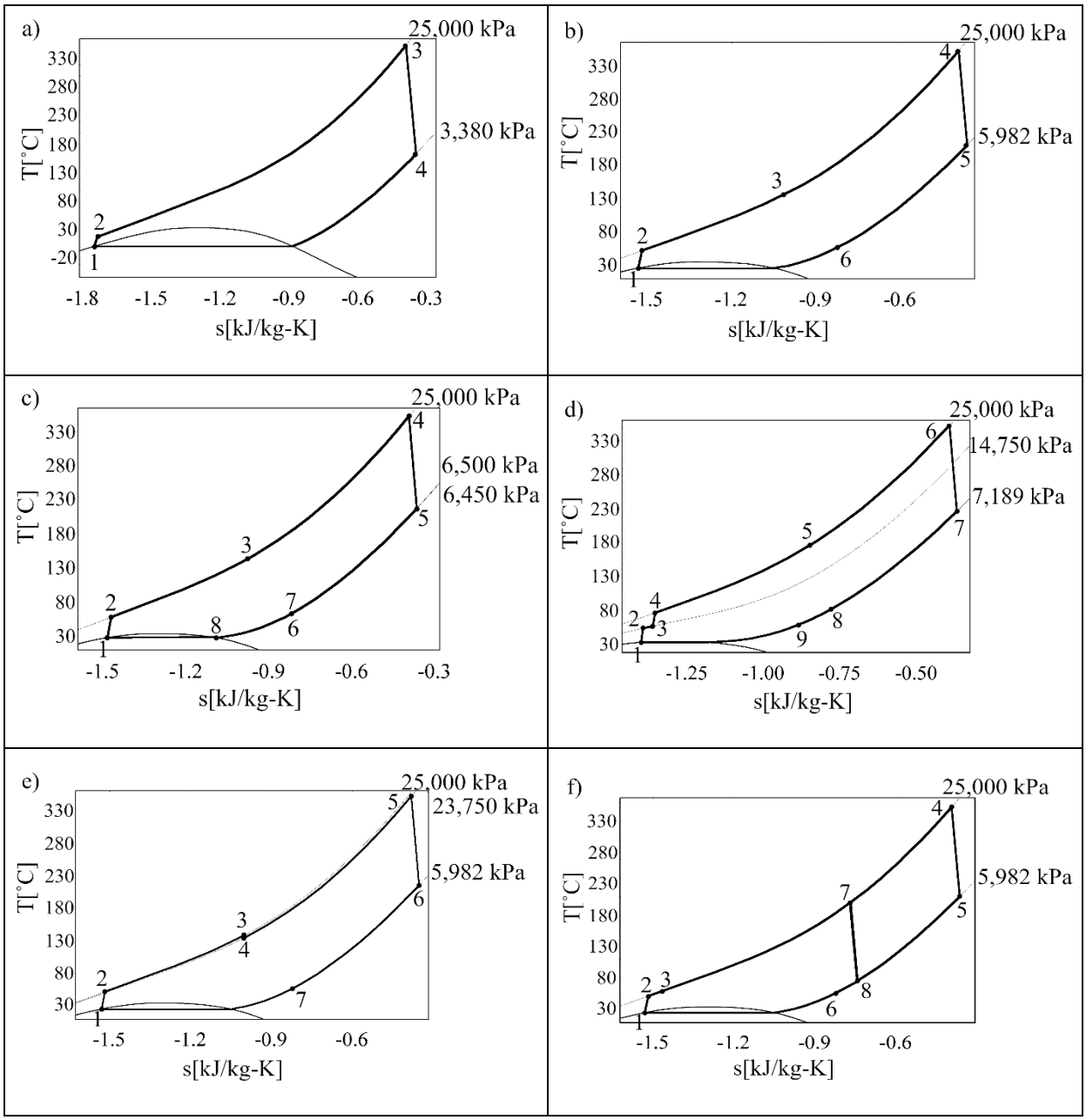

Figure 3.3: Temperature (T) – entropy (s) diagrams of the six transcritical CO_2 cycles assessed in this study. a, b, c, d, e, and f represent the basic cycle, regenerative cycle, intercooling cycle, inter-regenerative cycle, split-expansion cycle, and double-stage cycle, respectively.

3.2.3 Exergy analysis

An exergy analysis is performed on each power cycle configuration described in Section 3.2.2 to determine common sources of exergy destruction and identify potential areas where design improvements can be made.

For each cycle, the following exergy balance equation is applied to all components:

$$\frac{dE_x}{dt} = \sum_j \dot{E}_{xQj} - \dot{W} + \sum_i \dot{m} e_{xfi} - \dot{\Pi}_D \tag{3.11}$$

where $\frac{dE_x}{dt}$ is the rate of exergy change as a function of time (in kW), $\dot{E}_{xQ}$ is the exergy transfer accompanying heat transfer between the component casing and the environment (in kW), $\dot{W}$ is the exergy transfer accompanying work (in kW), e_{xf} is the specific exergy transfer accompanying fluid flow through the component (in kJ/kg), and $\dot{\Pi}_D$ is the exergy destruction rate (in kW). The subscripts j and i represent the number of inlets and outlets in any given component for the exergy transfer accompanying heat transfer and flow exergy, respectively.

Assuming all cycles operate at steady state and the exergy transfer accompanying heat transfer between the component casing and the environment is negligible, Equation 3.11 can be reduced and reorganized in the following form:

$$\dot{\Pi}_D = \sum_i \dot{m} e_{xfi} - \dot{W} \tag{3.12}$$

Table 3.1 demonstrates how the reduced exergy balance equation (*i.e.* Equation 3.12) is used to determine the rate of exergy destruction occurring in each component considered in the analysis.

Table 3.1: Application of reduced exergy balance equation to determine exergy destruction rate occurring in all components considered in the analysis. $\dot{m}_{hl}$ and $\dot{m}_{cl}$ represent the mass flow rate (in kg/s) of the working fluid in the heating and cooling loop respectively; $h_{hl,in}$, $h_{hl,out}$, $s_{hl,in}$, and $s_{hl,out}$ represent the real enthalpy (in kJ/kg) and entropy values (in kJ/kgK) of the working fluid entering and exiting the evaporator on the heating loop side, respectively; $h_{cl,in}$, $h_{cl,out}$, $s_{cl,in}$, and $s_{cl,out}$ represent the real enthalpy (in kJ/kg) and entropy values (in kJ/kgK) of the working fluid entering and exiting the condenser on the cooling loop side, respectively; $s_{in,t}$, $s_{out,t}$, $s_{in,p}$, $s_{out,p}$, $s_{in,c}$, $s_{out,c}$, $s_{in,e}$, and $s_{out,e}$ represent the entropy values (in kJ/kgK) of the working fluid entering and exiting the turbine, pump, condenser, and evaporator, respectively; and $s_{in,hot}$, $s_{out,hot}$, $s_{in,cold}$, $s_{out,cold}$ represent the entropy values (in kJ/kgK) of the working fluid entering and exiting the hot and cold sides of the regenerator, respectively. T_0 is the temperature at the dead state, and is assumed to be 298 K [68].

Component type	Reduced exergy balance equation	Component schematic
Evaporator	$\dot{\Pi}_D = \dot{m}_{hl}\left[\left(h_{hl,in} - h_{hl,out}\right) - T_0\left(s_{hl,in} - s_{hl,out}\right)\right] - \dot{m}\left[\left(h_{out,e} - h_{in,e}\right) - T_0\left(s_{out,e} - s_{in,e}\right)\right]$	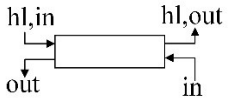
Turbine	$\dot{\Pi}_D = \dot{m}\left[\left(h_{in,t} - h_{out,t}\right) - T_0\left(s_{in,t} - s_{out,t}\right)\right] - \dot{W}_t$	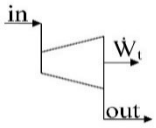
Condenser	$\dot{\Pi}_D = \dot{m}_{cl}\left[\left(h_{cl,in} - h_{cl,out}\right) - T_0\left(s_{cl,in} - s_{cl,out}\right)\right] - \dot{m}\left[\left(h_{out,c} - h_{in,c}\right) - T_0\left(s_{out,c} - s_{in,c}\right)\right]$	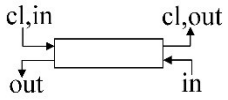
Pump	$\dot{\Pi}_D = \dot{m}\left[\left(h_{in,p} - h_{out,p}\right) - T_0\left(s_{in,p} - s_{out,p}\right)\right] + \dot{W}_p$	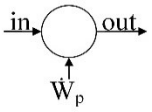
Regenerator	$\dot{\Pi}_D = \dot{m}\left[\left(h_{in,hot} - h_{out,hot}\right) - T_0\left(s_{in,hot} - s_{out,hot}\right)\right] - \dot{m}\left[\left(h_{out,cold} - h_{in,cold}\right) - T_0\left(s_{out,cold} - s_{in,cold}\right)\right]$	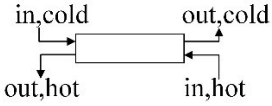

3.2.4 Performance metrics

Two metrics are used to quantify the thermodynamic performance of each power cycle considered in the analysis: the 1st law and 2nd law efficiencies. The 1st law efficiency demonstrates the extent to which heat is transformed into work for a given cycle and is expressed as

$$\eta_I = \frac{\dot{W}_{net}}{Q_{in}}. \tag{3.13}$$

The 2nd law efficiency represents the ratio of a given cycle's 1st law efficiency relative to the maximum theoretical efficiency that can possibly be attained (*i.e.* the Carnot efficiency). For all cycles, it is expressed as

$$\eta_{II} = \frac{\sum \dot{E}_{x,product}}{\sum \dot{E}_{x,input}} \tag{3.14}$$

where $\sum \dot{E}_{x,product}$ represents the sum of all useful exergy products, which is equivalent to $\dot{W}_{net}$, and $\sum \dot{E}_{x,input}$ represents the sum of all exergy inputs from both the evaporator and condenser. The latter parameter is calculated as follows:

$$\begin{aligned} \sum \dot{E}_{x,input} = \dot{m}_{hl}\left[\left(h_{hl,in} - h_{hl,out}\right) - T_0\left(s_{hl,in} - s_{hl,out}\right)\right] \\ + \dot{m}_{cl}\left[\left(h_{cl,in} - h_{cl,out}\right) - T_0\left(s_{cl,in} - s_{cl,out}\right)\right] \end{aligned} \tag{3.15}$$

3.2.5 Model verification

A verification of the thermodynamic modelling framework presented in Section 3.2.2 is performed by comparing the results of this study with those obtained from the literature. The double-stage transcritical CO_2 cycle demonstrated in Figure 3.3f is selected for this purpose. State points in the current model are modified slightly to correspond with the operating conditions detailed in Wu et al. [34]. Figures 3.4a to 3.4d show the temperature variation of three different state points, T_2, T_5, and T_8, in the cycle, and the net work output, $\dot{W}_{net}$, as T_4 is varied from 220 to 490 ˚C.

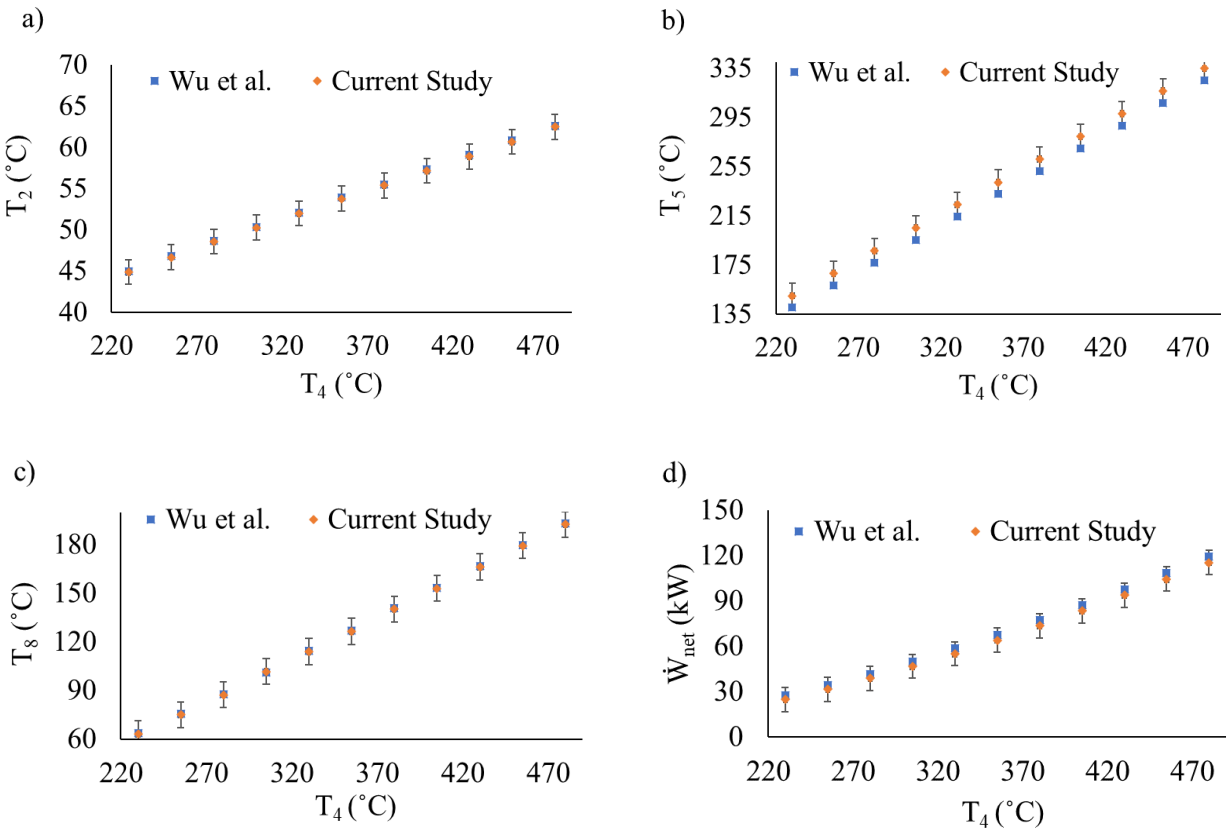

Figure 3.4: Variation in state point temperatures T_2, T_5, and T_8; and net work output, $\dot{W}_{net}$, for double-stage transcritical CO_2 cycle as a function of T_4. A comparison is shown between model outputs from the current study and data obtained from the literature for the same cycle [34].

For each data point value depicted in these figures, error bars corresponding to a range of ± 1.5% are shown. As all values fall within this minimal range, the modelling framework used in the current analysis is deemed verified.

3.2.6 Economic Analysis

An analysis is conducted to assess the economic viability of each power cycle configuration. For each configuration, the net present value (NPV) is calculated in Canadian dollars (CAD) using the following expression:

$$NPV = -c_c + \sum_j^k \frac{R_j - c_j}{(1+i)^j} \tag{3.16}$$

where c_c, R_j, c_j, i, j , and k represent the system's total capital cost (in CAD), annual revenue from electricity sales (in CAD/year), annual O&M cost (in CAD/year), effective interest rate, year, and project lifetime (in years), respectively. The total capital cost (in CAD) is expressed as

$$c_c = 1.07 * (c_{evap} + c_{regen} + c_{cond} + c_p + c_{turb}) \tag{3.17}$$

where c_{evap}, c_{regen}, c_{cond}, c_p and c_{turb} are the capital costs (in CAD) associated with the evaporator, regenerator, condenser, CO_2 pump, and turbine, respectively [69, 70]. Expressions corresponding to each of these terms are provided as follows:

$$c_{evap} = c_{regen} = 235 * {Q_{in}}^{0.75} \tag{3.18}$$

$$c_{cond} = 597 * {Q_{out}}^{0.68} \tag{3.19}$$

$$c_p = 451.37 * \dot{W}_p - 1769.7 \tag{3.20}$$

$$c_{turb} = -0.0207 * \dot{W}_t^2 + 665.5 * \dot{W}_t \tag{3.21}$$

The variables Q_{in}, Q_{out},$\dot{W}_p$, and $\dot{W}_t$ in the above equations represent the heat transferred to the evaporator or regenerator (in kW), the heat removed from the condenser (in kW), the pump work (in kW), and the turbine work (in kW), respectively, under nominal operating conditions. The first term on the right side of Equation 3.17 is included to further increase the total capital cost by 7% to account for the one-time installation cost of all components [71].

The annual O&M cost (in CAD/year) is assumed to be equal to 5% of the total capital cost [71]. The annual revenue from electricity sales (in CAD/year) is given by

$$R_j = \left(\sum \dot{W}_{out} - \sum \dot{W}_{in}\right) t * r \tag{3.22}$$

where $\dot{W}_{out}$ and $\dot{W}_{in}$ represent the total turbine work output (in kW), and total system work input (in kW), respectively. The total system work input is defined as the sum of the total CO_2 pump work input and the cooling loop chiller work input. The cooling loop chiller is assumed to have a COP of 3 [72]. The variables t and r in Equation 3.18 represent the annual cement plant operating hours (in hours/year) [14], and the per unit cost of electricity (in CAD/kWh), respectively. A value of 13.5 cents/kWh is assumed in the current study which is equivalent to the average rate paid for electricity in Canada [73].

All system components are assumed to have a lifetime of 35 years [69], and an effective interest rate of 8% [74]. Furthermore, it is assumed that the systems are built overnight, and the salvage value of the components is negligible. Finally, the capital cost of the heating and cooling loop components are not included in the economic analysis.

3.3 Results and discussion

Six transcritical CO_2 power cycles driven by waste heat from a cement plant are compared based on their thermodynamic and economic performance. The thermodynamic performance of each cycle is assessed via the system's 1st and 2nd law efficiency, whereas the economic performance is assessed via the system's NPV. Common sources of exergy destruction for these cycles are determined via the development of an exergy accounting framework, which is used to identify potential areas where design improvements can be made. The following insights are drawn from the analysis:

<u>Insight 1: Incorporating a regenerator to the basic transcritical CO_2 power cycle significantly increases the system's thermodynamic performance</u>

Figure 3.5 shows the 1st and 2nd law efficiencies corresponding to each of the six power cycles considered in this study.

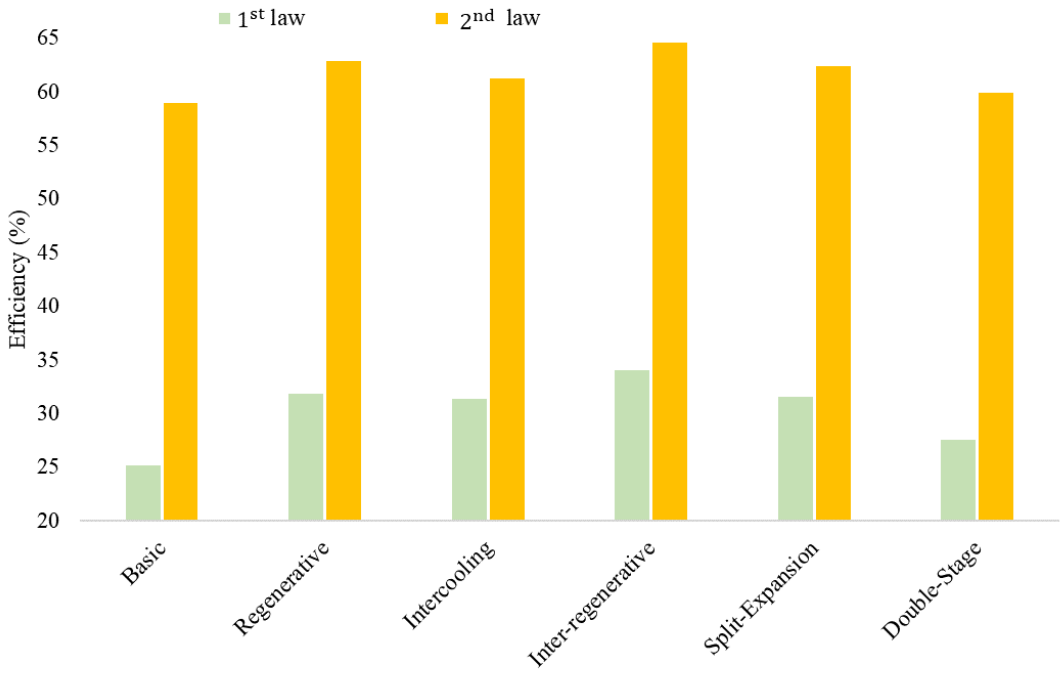

Figure 3.5: System 1st and 2nd law efficiencies of six transcritical CO_2 power cycles considered in this study.

The basic and double-stage cycles show the worst thermodynamic performance with 1st and 2nd law efficiencies of 25.2% and 59%, and 27.5% and 59.9%, respectively. The regenerative, intercooling, and split-expansion cycles show slightly better performance with 1st and 2nd law efficiencies of 31.9% and 62.9%, 31.4% and 61.2%, and 31.6% and 62.4%, respectively. The inter-regenerative cycle shows the best performance with 1st and 2nd law efficiencies of 34% and 64.5% respectively. Relative to the basic cycle, the 1st and 2nd law efficiencies of the inter-regenerative cycle are higher by roughly 8.8%, and 5.5%, respectively. These values correspond to an increase in net cycle power output of approximately 3.3 MW, as shown in Table 3.2. Although the inter-

regenerative cycle shows better thermodynamic performance than the basic cycle, it should be noted that its operation requires the use of two regenerators and two pumps in addition to the evaporator, condenser, and turbine, whereas the basic cycle only requires one pump in addition to these components. The requirement of these additional components (*i.e.* in the inter-regenerative cycle) may be a considerable barrier to implementation for these systems in cement plants as more complex power cycles typically require the use of more advanced instrumentation and control systems [57]. On the other hand, the 1st and 2nd law efficiencies of the regenerative cycle are greater than those of the basic cycle by approximately 6.7% and 3.9%, respectively. These values are only slightly lower than those shown for the inter-regenerative cycle and correspond to an increase in net cycle power output of approximately 2.5 MW, as shown in Table 3.1. Moreover, contrary to the inter-regenerative cycle, the regenerative cycle only requires one additional component than the basic cycle – a regenerator. This simple cycle arrangement, although inferior from a thermodynamic performance standpoint, presents clear benefits with regards to its feasibility of implementation in cement plants.

Insight 2: All six transcritical CO_2 power cycles analyzed in this study have thermodynamic performance values that are equivalent or better than those of conventional cycles used for waste heat recovery in cement plants

Figure 3.5 demonstrates that the 1st law efficiency for all six configurations varies from 25.2% for the basic cycle to 34% for the inter-regeneration cycle, and that the 2nd law efficiency varies from 59% to 64.5% for these same cycles, respectively. In a study by Wang et al. [28], which analyzes the thermodynamic performance of various power cycles driven by waste heat from a cement plant, results show 1st and 2nd law efficiencies of 25.7% and 42.1% for a single flash

steam cycle, 24.9% and 40.7% for a dual pressure steam cycle, 20.6% and 35.5% for an ORC utilizing R123 as a working fluid, and 24.1% and 43.0% for a Kalina cycle, respectively. Although direct comparisons cannot be made between the referenced study and the current study due to differences in assumed operating conditions, these values demonstrate that transcritical CO_2 power cycles are capable of operating with similar or better thermodynamic performance than cycles that are commonly used for this purpose in cement plant applications.

Insight 3: Condensers are the greatest single source of exergy destruction in every CO_2 power cycle considered

Figure 3.6 shows exergy flow schematics for the six transcritical CO_2 power cycles assessed in this study. The yellow, green, and blue arrows in this figure represent the flow exergy, exergy input/output, and exergy destruction streams (and associated quantities in kW) for each cycle, respectively. To ensure that all exergy input into the cycles is correctly accounted for, exergy accounting tables for each cycle are developed, and shown in Table 3.2. Table 3.2 shows that for all cycles, heat exchangers (*i.e.* evaporators, condensers, and regenerators) are responsible for the vast majority of exergy destruction. For each cycle, the exergy destruction in these components accounts for between 74% to 82% of the total exergy destroyed, with the lowest value being attributed to the inter-regenerative cycle and the highest value to the basic cycle. Of these components, the greatest amount of exergy destruction by far occurs in the condenser. For each cycle, the exergy destruction in the condenser(s) alone is responsible for between 43% and 52.2% of the total exergy destroyed, with the lowest value being attributed to the split-expansion cycle and the highest value to the inter-regenerative cycle. Focusing future

design efforts on improving the condenser is shown to offer the greatest potential for improving power cycle thermodynamic performance in all cases.

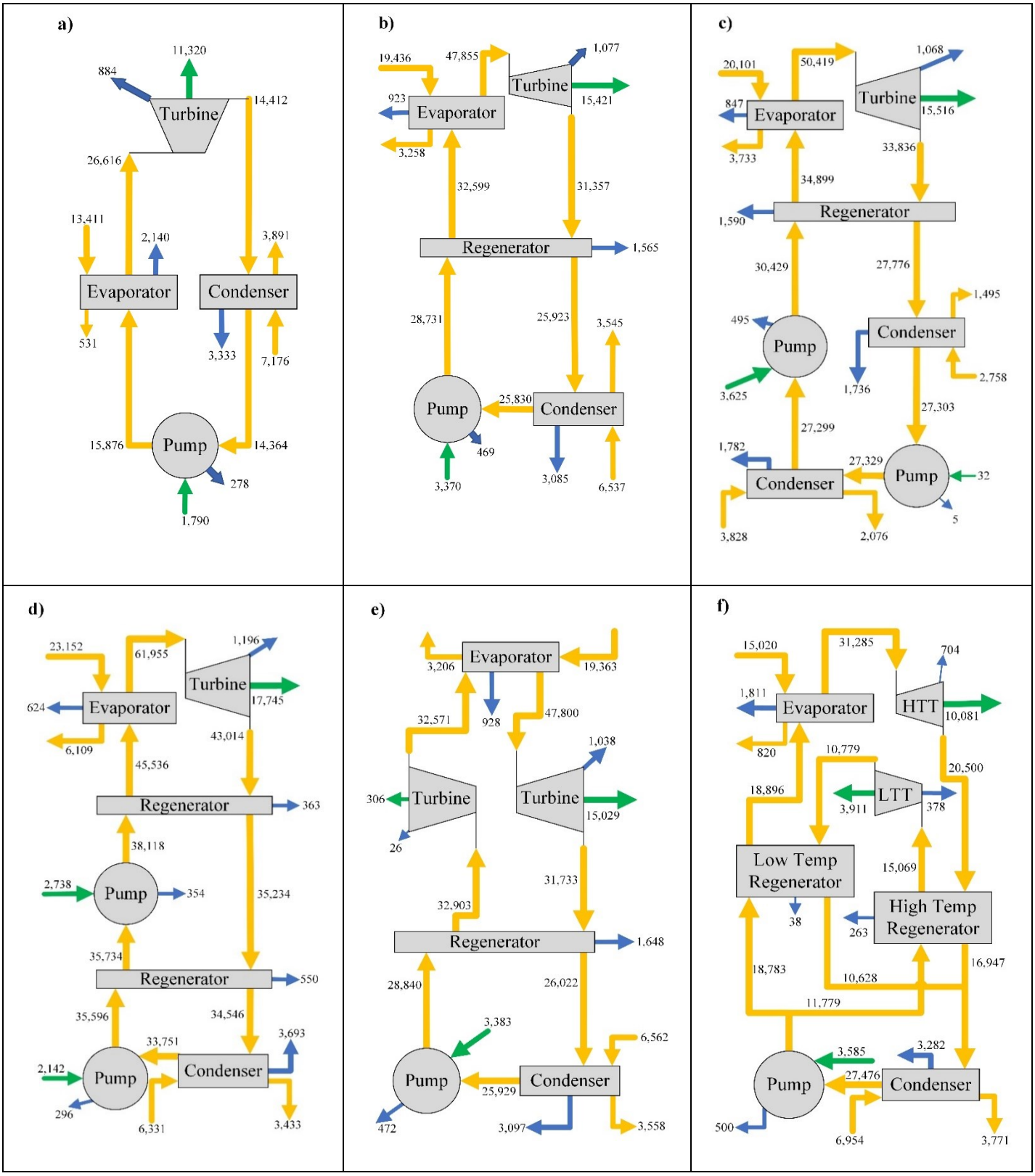

Figure 3.6: Exergy flow schematics of six transcritical CO_2 power cycles: a, b, c, d, e, and f represent the basic cycle, regenerative cycle, intercooling cycle, inter-regenerative cycle, split-expansion cycle, and double-stage cycle, respectively. For each cycle, yellow, green, and blue arrows represent flow exergy, exergy input/output, and exergy destruction streams, respectively. All quantities shown are in kW.

Table 3.2: Exergy accounting summaries of six transcritical CO_2 power cycles considered in this study.

	Basic cycle		Regenerative cycle		Intercooling cycle		Inter-regenerative cycle		Split-expansion cycle		Double-stage cycle	
Exergy Accounting	kW	%	kW	%	kW	%	kW	%	kW	%	kW	%
Net In												
Evaporator	12,880	72	16,178	72	16,368	71	17,043	69	16,157	72	14,200	68
Condenser 1	3,285	18	2,992	13	1,263	5	2,898	12	3,004	13	3,183	15
Condenser 2					1,752	8						
Pump 1	1,790	10	3,370	15	31	0	2,142	9	3,383	15	3,585	17
Pump 2					3,625	16	2,738	11				
Total	**17,955**	**100**	**22,540**	**100**	**23,039**	**100**	**24,821**	**100**	**22,544**	**100**	**20,968**	**100**
Net Out												
Turbine 1	11,320	63	15,421	68	15,516	67	17,745	71	306	1	10,081	48
Turbine 2									15,029	67	3,911	19
Destroyed												
Evaporator	2,140	12	923	4	847	4	624	3	928	4	1,811	9
Turbine 1	884	5	1,077	5	1,068	5	1,196	5	26	0	704	3
Turbine 2									1,038	5	378	2
Pump 1	278	2	469	2	5	0	296	1	472	2	500	2
Pump 2					495	2	354	1				
Condenser 1	3,333	19	3,085	14	1,736	8	3,693	15	3,097	14	3,282	16
Condenser 2					1,782	8						
Regenerator 1			1,565	7	1,590	7	363	1	1,648	7	263	1
Regenerator 2							550	2			38	0
Total	**17,955**	**100**	**22,540**	**100**	**23,039**	**100**	**24,821**	**100**	**22,544**	**100**	**20,968**	**100**

Insight 4: The inter-regenerative transcritical CO_2 power cycle has the highest net present value out of all cycles considered

Figure 3.7 shows the NPV of the six transcritical CO_2 power cycles assessed in this study. All cycles are shown to have a positive NPV except for the basic cycle and the double-stage cycle. These cycles have NPVs of – 11.7 MCAD and -3.1 MCAD, respectively. The inter-regenerative cycle, on the other hand, has the highest NPV at 36.9 MCAD. The main reason for the large

variation in NPV shown in Figure 3.7 is directly related to the net work output of each cycle. Cycles that have greater net work output acquire more revenue from electricity sales and are thus more profitable as a result. The thermodynamic performance of a given cycle therefore has a major impact on its economic viability, and although the former is important from a technical perspective, the latter is essential with regards to making decisions on whether or not a system can realistically be implemented in a cement plant.

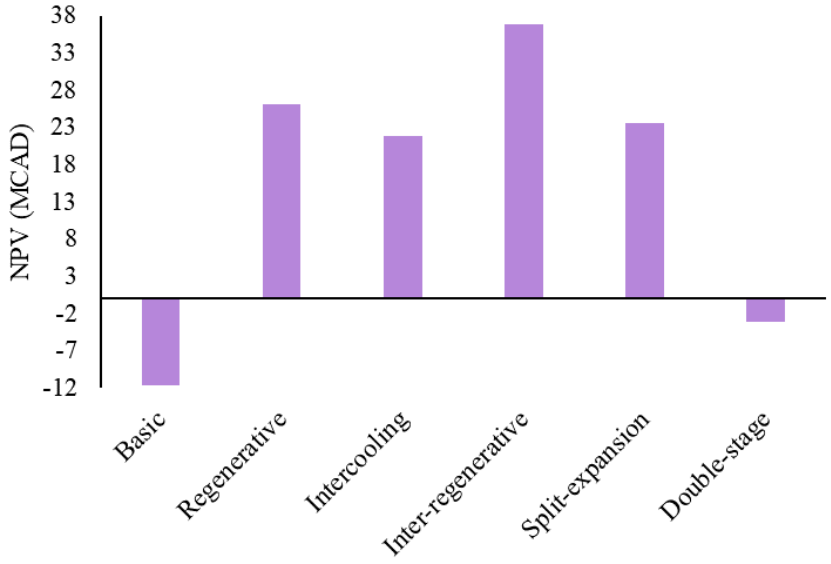

Figure 3.7: Net present value (NPV) of the six transcritical CO_2 power cycles assessed in this study.

Insight 5: The electricity price has the greatest single impact on the NPV of the inter-regenerative power cycle

A sensitivity analysis is conducted to identify the parameters used in the study that have the greatest impact on the system's net present value. The analysis is conducted on the cycle with the highest 1st and 2nd law performance - the inter-regenerative cycle, and the results are shown in Figure 3.8. The three following economic parameters are considered in the analysis: the electricity

price, the effective interest rate, and the component lifetime. For each parameter, the assumed value outlined in Chapter 3.2.6 is taken as the baseline value. The electricity price is varied from a "low value" of 11.5 cents (CAD)/kWh to a "high value" of 27 cents (CAD)/kWh, as per the range outlined in Chapter 3.2.6 [75]. The effective interest rate is varied from a "low value" of 4% to a "high value" of 12%, as these values correspond to average interest rates used in public and private sector projects in Canada, respectively [74]. Finally, the component lifetime is varied from 15 to 40 years, which is line with the minimum and maximum lifespan of the plant cycle components. An additional extreme case is also shown in Figure 3.8 for comparison, which combines "low" and "high" values from the above three economic parameters so as to obtain the lowest and highest possible NPV values, respectively.

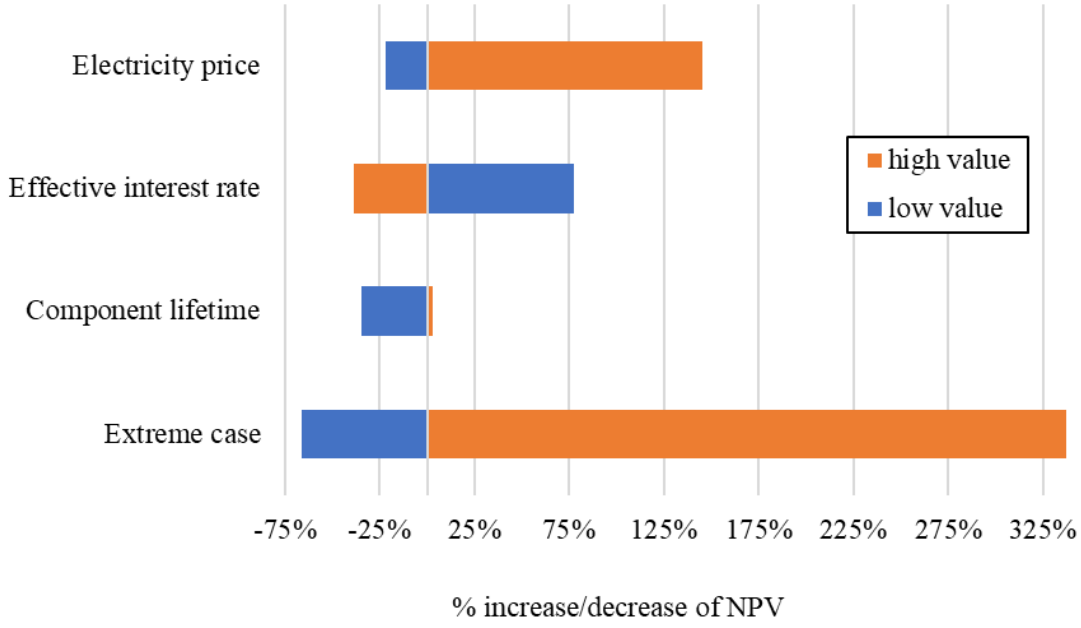

Figure 3.8: Sensitivity analysis showing % increase/decrease of NPV of inter-regenerative transcritical CO_2 power cycle from varying three key economic parameters (*i.e.* the electricity price, the effective interest rate, and the component lifetime) from the assumed value to both a high and a low value. An extreme case is also shown for comparison, which combines "low" and "high" values from the above three economic parameters so as to obtain the lowest and highest possible NPV values.

Figure 3.8 shows that decreasing and increasing the electricity price to the "low" and "high" value causes the NPV to decrease by 22% and increase by 145%, respectively. Similarly, decreasing and increasing the component lifetime to the "low" and "high" value causes the NPV to decrease by 34% and increase by 3%, respectively. However, the opposite effect is shown to occur for the effective interest rate as decreasing to the "low" value causes the NPV to increase by 78%, and increasing to the "high" value causes the NPV to decrease by 39%. When comparing the three parameters, the electricity price is shown to have the largest single impact on the NPV with an associated variation of approximately 167% between the "low" and "high" values. In the extreme case, however, this variation increases considerably to approximately 403%, with the greater part of the range being on the positive end of the spectrum. This finding demonstrates that given the uncertainties associated with assuming the economic parameters, there is a high likelihood that the NPV is greater than what has been determined using the baseline values. Moreover, even if the worst case is assumed (*i.e.* the "low value" of the extreme case), the NPV still has a positive value of 12.5 MCAD. Thus, regardless of the % decrease of NPV, the project remains profitable.

3.3.1 Limitations of the study

The following limitations have been identified with regards to the assumptions utilized in the current study:

- The heating and cooling loops are not modelled explicitly: this simplification may potentially lead to an overestimation of the thermodynamic and economic performance of each cycle as pumping energy and head losses in the piping are not accounted for.
- The heat transfer rate across the evaporator and condenser(s) is computed using a constant effectiveness value: To accurately gauge the thermodynamic performance of these

components, a more detailed analysis approach is recommended in which the heat transfer rate is computed directly as a function of the heat exchanger geometry and internal fluid flow characteristics.

- For all cycles, the energy transfer rate across the evaporator is fixed at 136.2 GJ/hr, and the temperature of the working fluid entering the evaporator from the heating loop is fixed at 355˚C: Since different cement plants emit different levels of waste heat across a wide range of temperatures, a sensitivity analysis is recommended to quantify the thermodynamic performance of each transcritical cycle as a function of heat availability, and the temperature of the heating loop working fluid.
- Head losses in the piping and components of each cycle are not considered: A more detailed analysis that includes these considerations would potentially increase the accuracy of estimating the overall thermodynamic performance.
- The economic feasibility of all cycles is calculated using a single set of assumptions: A sensitivity analysis is recommended to determine the economic viability of each cycle under varying conditions.

Addressing these limitations provides a good starting point for future research, which is described in Chapter 5.

3.4 Conclusion

Six transcritical CO_2 power cycles have been evaluated for recovering waste heat from a case study cement plant. These cycles include the basic, regenerative, intercooling, inter-regenerative, split-expansion, and double-stage cycles. It was found that the inter-regenerative cycle has the highest 1st and 2nd law efficiency, and that the regenerator is the primary component

responsible for increasing the cycle's thermodynamic performance relative to the basic cycle. It was also concluded that condensers are the greatest single source of exergy destruction, bringing to light the need to improve the design of this component in all cycles to boost thermal efficiency. In addition to the technical benefits listed above, the inter-regenerative cycle was found to have the highest net present value and is therefore the most cost-effective cycle of all the configurations considered. Furthermore, the inter-regenerative cycle is beneficial from an environmental standpoint as it emits the least amount of waste heat to the atmosphere. Given the large number of cement plants currently in operation worldwide, implementing these systems on a large scale has the potential to play an important role with regards to reducing society's impact on global warming.

Chapter 4: Summary of contributions

This thesis evaluates the technical, economic, and environmental performance of various power cycles comprising low global warming potential working fluids for low-grade waste heat recovery from data centers, and high-grade waste heat recovery from cement plants. A summary of the contributions from each chapter of this thesis are outlined below:

4.1 A techno-economic evaluation of low global warming potential heat pump assisted organic Rankine cycle systems for data center waste heat recovery

This chapter studied the thermodynamic performance of refrigerant-based HPA-ORC systems utilizing various low GWP refrigerants for WHR in data centers. An economic assessment of a HPA-ORC system was conducted and compared to a traditional ASHP chiller system, using three theoretical server utilization scenarios as inputs. The main findings are as follows:

- Low GWP working fluids demonstrate equal or better thermodynamic performance over conventional high GWP working fluids when used in a HPA-ORC system. This means that these systems can maintain their thermodynamic performance while greatly reducing their environmental impact.
- Low GWP working fluids can potentially replace conventional working fluids without major system modifications, since all working fluids considered operate under similar pressures and temperatures.
- Regardless of working fluid selection, the HPA-ORC WHR system is less costly than the conventional ASHP chiller system, as the HPA-ORC system produces electricity, providing a revenue stream to compensate for additional capital costs.

- As opposed to the ASHP chiller system, the profitability of the HPA-ORC system increases with an increase in server utilization. This demonstrates that for larger data centers, or data centers looking to expand, increasing server utilization with a HPA-ORC system will increase profitability, while the same scenario with an ASHP chiller system will have the opposite effect.
- HPA-ORC systems are a lower risk investment than ASHP chillers for WHR in data centers as their profitability increases with an increase in server utilization, which is likely to occur over the operating life of a data center. Moreover, HPA-ORC systems are less sensitive to changes in discount rates and electricity prices than ASHP chillers, which means that their current value is less likely to decrease with changing economic conditions.

4.2 A performance assessment of transcritical carbon dioxide power cycles driven by waste heat from cement plants

This chapter studied the thermodynamic and economic performance of six transcritical carbon dioxide power cycles for WHR in cement plants, with the intent of underlining ideal configurations or considerations for the application of these systems in this context. Both the energetic and exergetic efficiencies were used for the thermodynamic performance and the NPV of each configuration was used for the economic feasibility evaluation. The mains findings are as follows:

- The addition of a regenerator to a transcritical carbon dioxide power cycle used for WHR in cement plants greatly increases the system's thermodynamic performance, underlining the importance of this component when choosing a configuration for WHR in this context.

- The inter-regenerative configuration, with two regenerators, has the highest thermodynamic and economic performance, further demonstrating the positive impacts of regenerators in these systems. This performance leads to the lowest level of waste heat rejection into the atmosphere, rendering this configuration the most environmentally friendly as well.
- Condensers are the greatest source of exergy destruction in every configuration, demonstrating the need for efficient heat exchangers in this application.
- The electricity price has the greatest single impact on the NPV of the inter-regenerative power cycle, underlining the critical nature of this factor when implementing waste heat recovery systems.

Chapter 5: Recommendations and future work

Throughout this research project, several unresolved issues and limitations have been identified that warrant further study. These are discussed in detail at the end of chapters 2 and 3. This research project has also underlined several recommendations regarding potential areas for future work, which are provided below:

- In the current study, all working fluids were considered as a pure solution. However, refrigerants can be mixed to achieve different thermophysical properties. Further research into the mixture of low GWP working fluids for use in waste heat driver power cycles could result in better performance.
- As outlined in this thesis, heat exchangers are a significant source of energy loss in most power cycle configurations used for WHR applications, underlining the requirement for continued advancements in this field. Although outside of the scope of the research presented herein, further work regarding increasing the effectiveness of the heat exchangers used in these cycles could potentially have a significant impact on system performance.
- Multiple assumptions were made in order to model the systems described in this thesis. Greater accuracy of the modelling results could be achieved if a more detailed analysis approach were utilized that includes considerations such as head losses in the system piping and components, estimation techniques that compute the heat transfer rate in heat exchangers directly as a function of the heat exchanger geometry and internal fluid flow characteristics, and accurate component sizing.

Chapter 6: Conclusion

This thesis evaluated the possibilities for waste heat driven power cycles in various industrial sectors, based on the quality of the exhaust heat, to determine if more environmentally friendly options were thermodynamically and economically viable. In chapter 2, the thermodynamic performance of refrigerant-based HPA-ORC systems utilizing various low GWP refrigerants were investigated. An economic assessment was additionally conducted to assess the feasibility of these systems when compared to a traditional ASHP chiller system. It was found that certain low GWP working fluids, like R161 and pentane, have similar or better thermodynamic performance than conventional working fluids, like R134 and R245fa, when used in a HPA-ORC system. From an economic feasibility standpoint, it was determined that the HPA-ORC system is less costly than the ASHP chiller when operating under the same conditions for all working fluids considered. Moreover, the profitability of HPA-ORC systems increases with an increase in server utilization, while the opposite holds true for ASHP chiller systems. Both electricity price and discount rate have the greatest impact on the NPC of ASHP chiller systems, whereas capital cost and O&M costs have the greatest impact on the NPC of HPA-ORC configurations. Overall, the analysis showed that low GWP working fluids are a thermodynamically and economically viable alternative to conventional working fluids in data center HPA-ORC systems. Implementing these systems on a large scale has the potential to provide considerable benefits to an industry that is projected to continue growing along with our society's dependence on cloud-based IT services. In chapter 3, six transcritical CO_2 power cycles were evaluated for recovering waste heat from a case study cement plant. These cycles include the basic, regenerative, intercooling, inter-regenerative, split-expansion, and double-stage cycles. It was found that the inter-regenerative cycle has the

highest 1st and 2nd law efficiency, and that the regenerator is the primary component responsible for increasing the cycle's thermodynamic performance relative to the basic cycle. It was also concluded that condensers are the greatest single source of exergy destruction, bringing to light the need to improve the design of this component in all cycles to boost thermal efficiency. In addition to the technical benefits listed above, the inter-regenerative cycle was found to have the highest net present value and is therefore the most cost-effective cycle of all the configurations considered. Furthermore, the inter-regenerative cycle is beneficial from an environmental standpoint as it emits the least amount of waste heat to the atmosphere. Given the large number of cement plants currently in operation worldwide, implementing these systems on a large scale has the potential to play an important role with regards to reducing society's impact on global warming. Overall, it is believed that this and further research in this topic will encourage industries that emit large quantities of waste heat to implement waste heat driven power cycles that utilize environmentally friendly working fluids.

References

[1] C. Forman, I. K. Muritala, R. Pardemann and B. Meyer, "Estimating the global waste heat potential," *Renewable and Sustainable Energy Reviews,* no. 57, pp. 1568-1579, 2016.

[2] L. Miro, S. Bruckner and L. Cabeza, "Mapping and discussing Industrial Waste Heat (IWH) potentials for different countries," *Renewable and Sustainable Energy Reviews,* no. 51, pp. 847-855, 2015.

[3] L. Miro, R. McKenna, T. Jager and L. Cabeza, "Estimating the industrial waste heat recovery potential based on CO2 emissions in the European non-metallic mineral industry," *Energy Efficiency,* no. 11, pp. 427-443, 2018.

[4] I. Korolija and R. Greenough, "Modelling the Influence of Climate on the Performance of the Organic Rankine Cycle for Industrial Waste Heat Recovery," *Energies,* vol. 9, no. 335, 2016.

[5] M. Preissinger and D. Bruggemann, "Thermoeconomic Evaluation of Modular Organic Rankine Cycles for Waste Heat Recovery over a Broad Range of Heat Source Temperatures and Capacities," *Energies,* vol. 10, no. 269, 2017.

[6] A. Capozzoli and G. Primiceri, "Cooling Systems in Data Centers: State of Art and Emergin Technologies," *Energy Procedia,* vol. 83, pp. 484-493, 2015.

[7] International Energy Agency, "Digitalization and Energy," International Energy Agency, Paris, 2017.

[8] E. Samadiani, "Energy efficient thermal management of data centers via open multi-scale design," Georgia Institute of Technology, Georgia, 2009.

[9] J. Marcinichen, J. Olivier and J. Thome, "On-chip two-phase cooling of data centers: cooling system and energy recovery evaluation," *Applied Thermal Engineering,* vol. 41, pp. 36-51, 2012.

[10] M. Dayarathna, Y. Wen and R. Fan, "Data Center Energy Consumption Modeling: A Survey," *IEEE Communications Surveys & Tutorials,* vol. 18, no. 1, pp. 732-794, 2016.

[11] A. Haywood, J. Sherbeck, P. Phelan, G. Varsamopoulos and S. Gupta, "Thermodynamic feasibility of harvesting data center waste heat to drive an absoption chiller," *Energy Conversion Management,* vol. 58, pp. 26-34, 2012.

[12] B. Tchanche, G. Lambrinos, A. Frangoudakis and G. Papadakis, "Low-grade heat conversion into power using organic Rankine cycles - A review of various applications," *Renewable and Sustainable Energy Reviews,* vol. 15, no. 8, pp. 3963-3979, 2011.

[13] A. C. Kheirabadi and D. Groulx, "Cooling of server electronics: A design review of existing technology," *Applied Thermal Engineering,* vol. 105, pp. 622-638, 2016.

[14] Institute for Industrial Productivity, "Waste Heat Recovery for the Cement Sector: Market and Supplier Analysis," 2014.

[15] U.S. Department of Energy, "Waste Heat Recovery: Technology and Opportunities in U.S. Industry," 2008.

[16] J. Kline and C. Kline, "Assessing Cement Plant Thermal Performance," *IEEE TRANSACTIONS ON INDUSTRY APPLICATIONS,* vol. 53, no. 4, pp. 4097-4108, 2017.

[17] K. Ebrahimi, G. Jones and A. Fleischer, "A review of data center cooling technology, operating conditions and the corresponding low-grade waste heat recovery opportunities," *Renewable and Sustainable Energy Reviews,* vol. 31, pp. 622-638, 2014.

[18] K. Ebrahimi, G. Jones and A. Fleischer, "The viability of ultra low temperature waste heat recovery using organic Rankine cycle in dual loop data center applications," *Applied Thermal Engineering,* vol. 126, pp. 393-406, 2017.

[19] H. Yu, T. Gundersen and X. Feng, "Process integration of organic Rankine cycle (ORC) and heat pump for low temperature waste heat recovery optimal design," *Energy,* vol. 160, pp. 330-340, 2018.

[20] "Global warming potentials," 18 February 2019. [Online]. Available: https://www.canada.ca/en/environment-climate-change/services/climate-change/greenhouse-gas-emissions/quantification-guidance/global-warming-potentials.html. [Accessed 08 June 2019].

[21] I. Sarbu, "A review on substitution strategy of non-ecological refrigerants from vapour compression-based refrigeration, air-conditioning and heat pump systems," *International Journal of Refrigeration,* vol. 46, pp. 123-141, 2014.

[22] J. John, "Global Heat Pumps Market Expected To Reach USD 98.39 Billion By 2025: Zion Market Research," Zion Market Research, 17 April 2019. [Online]. Available: https://www.globenewswire.com/news-release/2019/04/17/1805406/0/en/Global-Heat-Pumps-Market-Expected-To-Reach-USD-98-39-Billion-By-2025-Zion-Market-Research.html. [Accessed 28 June 2019].

[23] Marketsandmarkets, "Heat Pump Market by Type (Air-to-Air and Air-to-Water), Rated Capacity (Up to 10 kW, 10–20 kW, 20–30 kW, and Above 30 kW), End-User (Residential, Commercial, and Industrial), and Region (North America, Europe, APAC, and RoW) - Global Forecast to 2023," Marketsandmarkets, 2018.

[24] E. Amiri Rad and S. Mohammadi, "Energetic and exergetic optimized Rankine cycle for waste hear recovery in a cement factory," *Applied Thermal Engineering,* no. 132, pp. 410-422, 2018.

[25] A. Ahmed, K. Khodary Esmaeil, M. A Irfan and F. Abdulrahman Al-Mufadi, "Design methodology of organic Rankine cycle for waste heat recovery in cement plants," *Applied Thermal Engineering,* no. 129, pp. 421-430, 2018.

[26] E. P. Barbosa Junior, M. D. Ponce Arrieta, F. R. Ponce Arrieta and C. H. Ferreira Silva, "Assessment of a Kalina cycle for waste heat recovery in the cement industry," *Applied Thermal Engineering,* no. 147, pp. 421-437, 2019.

[27] S. Karellas, A. Leontaritis, G. Panousis, E. Bellos and E. Kakaras, "Energetic and exergetic analysis of waste heat recovery systems in the cement industry," *Energy,* no. 58, pp. 147-156, 2013.

[28] J. Wang, Y. Dai and L. Gao, "Exergy analyses and parametric optimizations for different cogeneration power plants in cement industry," *Applied Energy,* no. 86, pp. 941-948, 2009.

[29] K. Ebrahimi, G. F. Jones and A. S. Fleischer, "The viability of ultra low temperature waste heat recovery using organic Rankine cycle in dual loop data center applications," *Applied Thermal Engineering,* vol. 126, pp. 393-406, 2017.

[30] P. Garg, P. Kumar, K. Srinivasan and P. Dutta, "Evaluation of isopentane, R-245fa and their mixtures as working fluids for organic Rankine cycles," *Applied Thermal Engineering,* vol. 51, pp. 292-300, 2013.

[31] M.-H. Yang and R.-H. Yeh, "Economic performances optimization of an organic Rankine cycle system with lower global warming potential working fluids in geothermal application," *Renewable Energy,* vol. 85, pp. 1201-1213, 2016.

[32] I. Sarbu, "A review on substitution strategy of non-ecological refrigerants from vapour compression-based refrigeration, air-conditioning and heat pump systems," *International Journal of Refrigeration,* vol. 46, pp. 123-141, 2014.

[33] J. Sarkar, "Review and future trends of supercritical CO2 Rankine cycle for low-grade heat conversion," *Renewable and Sustainable Energy Reviews,* no. 48, pp. 434-451, 2015.

[34] C. Wu, X.-j. Yan, S.-s. Wang, K.-l. Bai, J. Di, S.-f. Cheng and J. Li, "System optimisation and performance analysis of CO2 transcritical power cycle for waste heat recovery," *Energy,* no. 100, pp. 391-400, 2016.

[35] Y. Ma, Z. Liu and H. Tian, "A review of transcritical carbon dioxide heat pump and refrigeration cycles," *Energy,* no. 55, pp. 156-172, 2013.

[36] O. Olumayegun and M. Wang, "Dynamic modelling and control of supercritical CO2 power cycle using waste heat from industrial processes," *Fuel,* no. 249, pp. 89-102, 2019.

[37] O. Kizilkan, "Performance assessment of steam Rankine cycle and sCO2 Brayton cycle for waste heat recovery in a cement plant: A comparative study for supercritical fluids," *International Journal of Energy Research,* pp. 1-15, 2020.

[38] G.-B. Wang and X.-R. Zhang, "Thermoeconomic analysis of optimization potential for CO2 vapor compression cycle: From transcritical to supercritical operation for waste heat recovery from the steam condenser," *International Journal of Energy Research,* vol. 43, pp. 297-312, 2018.

[39] "Engineering Equation Solver," F-Chart Software, 2019. [Online]. Available: http://www.fchart.com/ees/. [Accessed 31 May 2019].

[40] F. S. da Silva and J. A. Matelli, "Exergoeconomic analysis and determination of power cost in MCFC - steam turbine combined cycle," *International Journal of Hydrogen Energy,* vol. 44, no. 33, pp. 18293-18307, 2019.

[41] B. Singh and P. Sahoo, "Modelling and simulation of a bio-fuelled conventional engine," *International Journal of Ambient Energy,* vol. 34, no. 4, pp. 200-213, 2013.

[42] G. R. Ahmadi and D. Toghraie, "Energy and exergy analysis of Montazeri Steam Power Plant in Iran," *Renewable and Sustainable Energy Reviews,* vol. 56, pp. 454-463, 2016.

[43] L. Garousi Farshi, S. Khalili and A. Mosaffa, "Thermodynamic analysis of a cascaded compression – Absorption heat pump and comparison with three classes of conventional heat pumps for the waste heat recovery," *Applied Thermal Engineering,* vol. 128, pp. 282-296, 2018.

[44] E. Bellos and C. Tzivanidis, "Parametric analysis and optimization of a solar driven trigeneration system based on ORC and absorption heat pump," *Journal of Cleaner Production,* vol. 161, pp. 493-509, 2017.

[45] D. Luo, A. Mahmoud and F. Cogswell, "Evaluation of low-GWP fluids for power generation with organic Rankine cycle," *Energy,* vol. 85, pp. 481-488, 2015.

[46] K. Satanphol, W. Pridasawas and B. Suphanit, "A study on optimal composition of zeotropic working fluid in an organic Rankine cycle (ORC) for low grade heat recovery," *Energy,* vol. 123, pp. 326-339, 2017.

[47] V. Le, M. Feidt, A. Kheiri and S. Pelloux-Prayer, "Performance optimization of low temperature power generation by supercritical ORCs (organic Rankine cycles) using low GWP (global warming potential) working fluids," *Energy,* vol. 67, pp. 513-526, 2014.

[48] Y. Wu, "Study of R161 refrigerant for residential air-conditioning applications," 2012.

[49] "Pentane," National Center for Biotechnology Information, [Online]. Available: https://pubchem.ncbi.nlm.nih.gov/compound/Pentane. [Accessed 09 June 2019].

[50] M. Moran and H. Shapiro, Fundamentals of engineering thermodynamics, 5th ed., John Wiley & Sons inc, 2004.

[51] J. Yogendra and K. Pramod, Energy Efficient Thermal Management of Data Centers, 2012.

[52] K. Choo, R. M. Galante and M. M. Ohadi, "Energy consumption analysis of a medium-size primary data center in an academic campus," *Energy and Buildings,* no. 76, pp. 414-421, 2014.

[53] L. Barroso and U. Hölzle, "The case for energy-proportional computing," *Computer,* vol. 40, no. 12, pp. 33-37, 2007.

[54] "Air-source heat pumps," 27 March 2017. [Online]. Available: https://www.nrcan.gc.ca/energy/publications/efficiency/heating-heat-pump/6831. [Accessed 25 June 2019].

[55] Treasury Board of Canada Secretariat, "Canadian Cost-Benefit Analysis Guide: Regulatory Proposals," 2007.

[56] Independent Electricity System Operator, "Annual Planning Outlook," Independent Electricity System Operator, 2020.

[57] G. Liao, L. Liu, J. E, F. Zhang, J. Chen, Y. Deng and H. Zhu, "Effects of technical progress on performance and application of supercritical carbon dioxide power cycle: A review," *Energy Conversion and Management,* no. 199, 2019.

[58] S.-s. Wang, C. Wu and J. Li, "Exergoeconomic analysis and optimization of single-pressure single-stage and multi-stage CO2 transcritical power cycles for engine waste heat recovery: A comparative study".

[59] L.-h. Zhang, L.-j. Wu, X.-h. Zhang and G.-d. Ju, "Comparison and optimization of mid-low temperature cogeneration systems for flue gas in iron and steel plants," *Journal of Iron and Steel Research,* vol. 20, no. 11, pp. 33-40, 2013.

[60] I. Girgin and C. Ezgi, "Design and thermodynamic and thermoeconomic analysis of an organic Rankine cycle for naval surface ship applications," *Energy Conversion and Management,* vol. 148, pp. 623-634, 2017.

[61] A. Nemati, H. Nami, F. Ranjbar and M. Yari, "A comparative thermodynamic analysis of ORC and Kalina cycles for waste heat recovery: A case study for CGAM cogeneration system," *Case Studies in Thermal Engineering,* vol. 9, pp. 1-13, 2017.

[62] H. Riyanto and S. Y. Martowibowo, "Optimization of organic Rankine cycle waste heat recovery for power generation in a cement plant vis response surface methodology," *International Journal of Technology,* no. 6, pp. 938-945, 2015.

[63] Y. M. Kim, J. L. Sohn and E. S. Yoon, "Supercritical CO2 Rankine cycles for waste heat recovery from gas turbine," *Energy,* vol. 118, pp. 893-905, 2017.

[64] D. Colorado, J. Hernandez and W. Rivera, "Comparative study of a cascade cycle for simultaneous refrigeration and heating operating with ammonia, R134a, butane, propane, and CO2 as working fluds," *International Journal of Sustainable Energy,* vol. 31, no. 6, pp. 365-381, 2012.

[65] R. V. Padilla, Y. C. Soo Too, R. Benito and W. Stein, "Exergetic analysis of supercritical CO2 Brayton cycles integrated with solar central receivers," *Applied Energy,* no. 148, pp. 348-365, 2015.

[66] S. Mondal and S. De, "CO2 based power cycle with multi-stage compression and intercooling for low temperature waste heat recovery," *Energy,* no. 90, pp. 1132-1143, 2015.

[67] E. Cayer, N. Galanis, M. Desilets, H. Nesreddine and P. Roy, "Analysis of a carbon dioxide transcritical power cycle using a low temperature source," *Applied Energy,* no. 86, pp. 1055-1063, 2009.

[68] P. Mago, K. Srinivasan, L. Chamra and C. Somayaji, "An examination of exergy destruction in organic Rankine cycles," *International Journal of Energy Research,* no. 32, pp. 926-938, 2008.

[69] J.-Y. Kim, S. Salim, J.-M. Cha and S. Park, "Development of Total Capital Investment Estimation Module for Waste Heat Power Plant," *Energies,* no. 12, 2019.

[70] M. Usman, M. Imran, Y. Yang, D. Hyun Lee and B.-S. Park, "Thermo-economic comparison of air-cooled and cooling tower based Organic Rankine Cycle (ORC) with R245fa and R1233zde as candidate working fluids for different geographical climate conditions," *Energy,* no. 123, pp. 353-366, 2017.

[71] M. Deymi-Dashtebayaz and S. Valipour-Namanlo, "Thermoeconomic and environmental feasibility of waste heat recovery of a data center using air source heat pump," *Journal of Cleaner Production,* no. 219, pp. 117-126, 2019.

[72] R. Chebbi, M. Qasim, N. Darwish and M. T. Ashraf, "Optimization and cost-oriented comparios of ammonia and propane-compression refrigeration for the recovery of natural gas liquids," *Energy Technology,* vol. 1, pp. 573-580, 2013.

[73] R. Urban, "Electricity Prices in Canada 2020," energyhub.org, 2020. [Online]. Available: https://energyhub.org/wp-content/uploads/Electricity-Prices-in-Canada-2020.pdf. [Accessed 19 October 2020].

[74] T. B. o. C. Secretariat, "Canadian Cost-Benefit Analysis Guide: Regulatory Proposals," Government of Canada, Ottawa, 2007.

[75] International Energy Agency, "Energy Prices 2020," International Energy Agency, 2020.